# Supplemental Material for "Marine Mammal Microbiota Yields Novel Antibiotic with Potent Activity Against *Clostridium difficile*"

Jessica L. Ochoa[1], Laura M. Sanchez[1,2], Byoung-Mo Koo[3], Jennifer S. Doherty[3], Manohary Rajendram[4], Kerwyn Casey Huang[4,5], Carol A. Gross[3], Roger G. Linington[1,6,*]

**Supplemental Table of Contents**

## Supplementary Materials

### Phylogenetic Analysis

Evolutionary history was inferred by using the maximum likelihood method based on the Tamura-Nei model.[1] The bootstrap consensus tree inferred from 2000 replicates was taken to represent the evolutionary history of the taxa analyzed. Branches corresponding to partitions reproduced in less than 50% of bootstrapped replicates were collapsed. The percentage of replicate trees in which the associated taxa clustered together in the bootstrap test (2000 replicates) are shown next to the branches (Fig. S1).[2,3] Initial tree(s) for the heuristic search were obtained automatically by applying Neighbor-Join and BioNJ algorithms to a matrix of pairwise distances estimated using the Maximum Composite Likelihood approach, and then selecting the topology with superior log-likelihood value. The analysis involved 44 nucleotide sequences. Codon positions included were 1st+2nd+3rd+Noncoding. All positions containing gaps and missing data were eliminated. There was a total of 1195 positions in the final dataset. Evolutionary analyses were conducted in MEGA5.[4]

### Extraction of Cultivated Isolates

Purified bacterial colonies were grown in 1 L of modified SYP broth (1 L Milli-Q water, 32.1 g Instant Ocean™, 10 g starch, 4 g peptone, 2 g yeast extract) with 20 g of Amberlite XAD-16 resin for 10 days at 27 °C. Culture broth and resin slurries were filtered through glass microfiber filters, washed with water (3×200 mL), and the cells, resin, and filter paper were extracted with 1:1 methanol/dichloromethane (250 mL). Organic fractions were dried *in vacuo* and subjected to solid phase extraction using Supelco-Discovery $C_{18}$ cartridges (5 g), eluting with a step gradient of 40 mL MeOH/$H_2O$ solvent mixtures (10%, 20%, 40%, 60%, 80%, 100% MeOH) and finally with EtOAc to afford seven fractions. The resulting fractions were dried *in vacuo*, resolubilized in 500 µL of dimethyl sulfoxide (DMSO), and transferred to deep-well 96-well plates for screening.

### Fermentation and Isolation

The producing organism, MMA 6B HVS/10A, was isolated from the lower intestine of a harbor porpoise (specimen LMLPP2011SEP29) under permit number 151408SWR2011PR00001:SMW. The strain was originally isolated on HVS medium (18 g agar, 50 mg nalidixic acid, 50 mg cycloheximide, 10 g starch, 1.7 g KCl, 0.01 g $FeSO_4 \cdot 7H_2O$, 0.5 g $MgSO_4 \cdot 7H_2O$, 0.5 g $Na_2PO4$, 3.0 g $KNO_3$, 0.5 mg thiamine (vitamin B1), 0.5 mg riboflavin (vitamin B2), 0.5 mg nicotonic acid (vitamin B3), 0.5 mg pyridoxine HCl (vitamin B6), 0.5 mg *p*-aminobenzoic acid, 0.5 mg myoinositol, 0.25 mg biotin, 20 mg $CaCO_3$, 750 mL 0.2-µm filtered seawater, 250 mL Milli-Q $H_2O$). All vitamins were dissolved in stock solutions, filtered, and added after autoclaving. Frozen stocks of environmental isolates were grown on fresh Marine Broth plates (37.4 g Difco Marine Broth, 18 g agar, 1 L Milli-Q water) and incubated at 25 °C until discrete colonies became visible. Selected colonies were inoculated into 10 mL modified saline SYP (mSYP) media

(10 g starch, 4 g peptone, 2 g yeast extract, 31.2 g Instant Ocean in 1 L distilled $H_2O$). The cultures were stepped up in stages at 7-day intervals by first inoculating 1.5 mL of the 10-mL cell cultures into 50 mL mSYP (medium scale), followed by inoculation of 40 mL of these medium-scale cell cultures into 1 L of the same broth also containing 20.0 g Amberlite XAD-16 adsorbent resin in 2.8 L Fernbach flasks for 7 days. All cultures were incubated at 25 °C containing glass beads for 10 mL cultures and stainless steel springs for 50 mL and 1 L cultures, and shaken at 200 rpm.

The cells and resin were collected from the bacterial extract by vacuum filtration using Whatman glass microfiber filters and washed with deionized water. This cell/resin slurry was extracted with 250 mL of 1:1 $MeOH/CH_2Cl_2$, and the organic extract was removed by vacuum filtration and concentrated to dryness *in vacuo*. The crude organic extract (code RLFI1036) was subjected to solid-phase extraction using a Supelco-Discovery C18 cartridge (10 g) and eluted using a step gradient of 80 mL $MeOH/H_2O$ solvent mixtures (10% MeOH (A), 20% MeOH (B), 40% MeOH (C), 60% MeOH (D), 80% MeOH (E), 100% MeOH (F), and finally ethyl acetate (G)) to afford seven fractions designated as A−G. The seven fractions were dried *in vacuo*. The 100% MeOH prefraction, RLUS1036F, was subjected to reverse-phase HPLC (Phenomenex Synergi Fusion-RP 5 µm, 80 Å, 250×4.6 mm, 65:35 $MeOH/H_2O$ isocratic run over 20 min, 1 mL/min flow rate) to produce phocoenamicin, which eluted at 15.7 min.

**Flow Cytometry**

Membrane potential was analyzed on a Becton Dickinson LSRII flow cytometer using the reagents and protocol from the BacLight™ Bacterial Membrane Potential Kit (B34950).

**Bacterial Strains**

Gram-positive: *Bacillus subtilis* 168*,* methicillin-susceptible *Staphylococcus aureus* (MSSA, ATCC 29213), *Staphylococcus epidermidis (*ATCC 14990) methicillin-resistant *Staphylococcus aureus* (MRSA, BAA-44), *Listeria ivanovii* (BAA-139), *Enterococcus faecium* (ATCC 6569), *Clostridium difficile* (ATCC 700057).

Gram-negative: *Escherichia coli* BW25113, *Providencia alcalifaciens* (ATCC 9886), *Ochrobactrum anthropi* (ATCC 49687), *Enterobacter aerogenes* (ATCC 35029), *Acinetobacter baumanii* (NCIMB 12457), *Vibrio cholerae* O1 biotype El Tor A1552, *Salmonella enteria* serovar Typhimurium LT2, *Pseudomonas aeruginosa* (ATCC 27853), *Yersinia pseudotuberculosis* (IP2666 pIBI).

**High-Throughput Antibacterial Inhibition Assay**

Bacterial test strains were grown on fresh agar plates and individual colonies were used to inoculate 3 mL sterile media. All *Staphylococcus* strains were grown in tryptic soy agar (TSA; 17 g tryptone, 3 g soytone, 2.5 g dextrose, 5 g NaCl, and 2.5 g dipotassium phosphate in 1 L distilled water; pH 7.5). *P. alcalifaciens*, *O. anthropi*, *E. aerogenes*, and *A. baumanii* were grown in nutrient broth agar (Difco, USA), and *B. subtilis*, *E. coli*, *V. cholerae*, *S.* Typhimurium, *P. aeruginosa*, and *Y. pseudotuberculosis* cultures were grown in Luria

Broth (10 g tryptone, 5 g yeast extract, and 10 g NaCl in 1 L distilled water; pH 7.5). *C. difficile* was grown on TSA plates supplemented with 5% sheep blood (Hardy Diagnostics, VWR catalog number 89405-024). All *C. difficile* media were placed in anaerobic chambers 24 h prior to inoculation, and all culture conditions were made anaerobic using disposable chambers (BD Diagnostics, 90003-642). All in-house media were autoclaved at 121 °C for 30 min. Antimicrobial MICs were determined using Mueller Hinton Broth (VWR catalog number 90003-966). Inoculated cultures were grown overnight with shaking (200 rpm, 30 °C). Saturated overnight cultures were diluted 1:10,000, 1:1000, or 1:100 according to turbidity and dispensed into sterile clear polypropylene 384-well plates (30 μL screening volume). Optical density ($OD_{600}$) of cultures at a 1:100 dilution was recorded (Shimadzu UV-Visible Spectrophotometer), and cultures were further diluted on agar plates to calculate colony forming units (CFU) per milliliter of culture. DMSO solutions of test compounds (200 nL) were pinned into each well prior to inoculation using a high-throughput pinning robot (Perkin Elmer Janus MDT). In the 384-well plates, lanes 1 and 2 were reserved for DMSO vehicle negative controls, while lanes 23 and 24 contained only culture medium and test organisms. After compound addition, screening plates were stacked in an automated plate reader/shaker (Perkin Elmer EnVision) and $OD_{600}$ was measured every 1 h for ~18 h. The resulting growth curves for each dilution series were used to determine MIC values for all test compounds following standard procedures.

**Structure Elucidation**

***Characterization of Phocoenamicin.*** White amorphous powder, $[\alpha]^{25}_{D}$ = -6.3, (c = 1.0, Acetone); UV(MeOH) $\lambda_{max}$ (log $\epsilon$) 232(3.34), 398(2.89), 314(2.82) nm; $^{1}H$ and $^{13}C$ see NMR table; HRMS $[M-H]^-$ 1069.4571 (calculated for $C_{56}H_{74}ClO_{18}$, 1069.4564)

***Subunit A (Glycosylation).*** Initial evaluation of the $^{1}H$ and $^{13}C$ spectra, coupled with HRMS data, suggested a molecular formula of $C_{56}H_{75}ClO_{18.}$ Examination of the HSQC spectrum suggested the presence of an aliphatic core, two sugar moieties, and a poly-substituted aromatic substituent (Fig. S3A). Evaluation of the COSY spectrum starting from the anomeric proton at 4.41 revealed a 6-deoxy-hexose sugar.

HMBC from δH 3.45 ppm on C3' to a new anomeric carbon C1" indicated a 1,3-linkage to a second sugar subunit. COSY correlations from this anomeric proton δH 4.61 on C1" revealed the presence of a second 6-deoxy-hexose sugar unit. HMBC from the proton at the 4 position (δH 4.93 on C4") to a new quaternary carbon C7" suggested the presence of a terminal substituent attached 1-4 to this sugar unit. HMBC correlations from δH 4.93 on C4" in the second sugar to the carbonyl C7" indicated an acetyl linkage to the aromatic core. HMBC correlations between aromatic proton δH 6.85 to C7" also confirmed the linkage. COSY correlations suggested adjacent aromatic protons. Comparison of $^{13}C$ chemical shifts to the known aromatic subunit of chlorothricin (Fig. S3C) as well as synthetic analogues of the aromatic core confirmed the regiochemistry of the ring. Together, these data identified subunit A.

## Configurational Analysis

Based on the analyses described within the main text and the supplementary the configuration of the stereogenic centers was found as follows: (4R, 5R, 6S, 8R, 9S, 10S, 13S, 14R, 18R, 21R, 23S*, 32S, 33R, 1'S, 2'R, 3'S, 4'R, 5'R, 1"S, 2"R, 3"S, 4"R, 5"R).

***Sugars.*** Relative configuration determined by ROE and $^{3}J_{HH}$ (approximate coupling constants were derived from the DQF-COSY). Key ROE correlations are represented in S3A. ROE correlations between H1' and H5' assigned them as axial protons on the top face of the sugar. Reciprocal ROE correlations between the methyl at C6' and both substituents on C4' (H4' & the δH 3.92 OH) suggested that the methyl was in the equatorial position, confirming the axial position of H5'. A large coupling constant of approximately 10 Hz between H5' and H4' set H4' as an axial proton on the bottom face of the sugar. A smaller coupling constant of approximately 4 Hz between H4' and H3' and a corresponding ROE placed H3' in the bottom face of the sugar. A coupling of approximately 5 Hz between H3' and H2' when considered with the ROE between H2' and H1' assigned H2' to the top face of the molecule in an equatorial position, completing the sugar composed of C1' to C6'. For the sugar containing C1" to C6" ROE correlations from H1" to H2" and H5" defined the top face. ROE correlations from H4" to H3" and H6" defined the bottom face.

***Synthesis of D-Glucopyranoside, methyl 6-deoxy-, 2,3,4-triacetate.*** Phocoenamicin (10 mg, 0.009 mmol) was subjected to methanolysis by refluxing in 4 mL 1N HCl:MeOH for 2 h. Upon cooling, the reaction mixture was concentrated to dryness *in vacuo* and partitioned between $H_2O$ (10 mL) and $Et_2O$ (10 mL). The phases were separated and the aqueous phase extracted with $Et_2O$ (2x 10 mL). The aqueous portion was lyophilized to dryness. To a mixture of the crude lyopholized product (1 mg) and $Y(CF_3SO_3)_3$ (0.1 mg) in dry DCM (5 mL) was added acetic anhydride (190 mL) at room temperature. After stirring for 2 h, the solution was quenched with saturated sodium bicarbonate solution, and the product was extracted with DCM three times. The combined organic extracts were washed with water and brine. The triacetate was purified using a Waters mass-directed preparative system equipped with an XBridge BEH130 5 μM 19 x 150 C18 column eluting with $H_2O$/acetonitrile. Triacetate 6-deoxy-D-glucopyranose was also synthesized from 6-deoxyglucopyranose using identical procedures. Optical rotation of the β anomer was consistent with synthetic compound β-D-Glucopyranoside, methyl 6-deoxy-, 2,3,4-triacetate (natural product): $[\alpha]^{25}_{D}$ = -4.2, (c =0.1, Chloroform), β-D-Glucopyranoside, methyl 6-deoxy-, 2,3,4-triacetate (synthetic standard): $[\alpha]^{25}_{D}$ = -4.7, (c =0.1, Chloroform).

## Cytological Profile Screening and Image Analysis

Methods for cell culture and staining were as previously reported (36, 37). HeLa cells were plated into two clear-bottom 384-well plates at a target density of 2,500 cells per well. The plates were incubated for 24 h under 5% $CO_2$ at 37 °C, 150 nL of extract was pinned onto the culture plates, and the plates were incubated for 19 h under 5% $CO_2$ at 37 °C. The plates were then fixed and stained with sets of either cell-cycle or cytoskeletal stains, which report on the number of cells in S-phase or mitosis and the amount and distribution of tubulin and

actin, respectively. Both stain sets also contained a nuclear stain (Hoechst), which was used to count the number of cells and segment the image. The plates were imaged with a 10X objective lens, acquiring four images per well. For each extract, 248 different parameters were measured from the images of each plate. Together, these values report on a diverse range of size and shape features, such as the total area and shape of the nuclei and the number of mitotic cells. Comparing extract-treated and DMSO-treated wells and reduction of these cellular metrics to population values for each well using a custom data management pipeline produced a 248-parameter fingerprint for each extract with attributes scaled from -1 to 1 (Fig. S4B).

**Fig. S1. Molecular phylogenetic analysis by maximum likelihood method.**

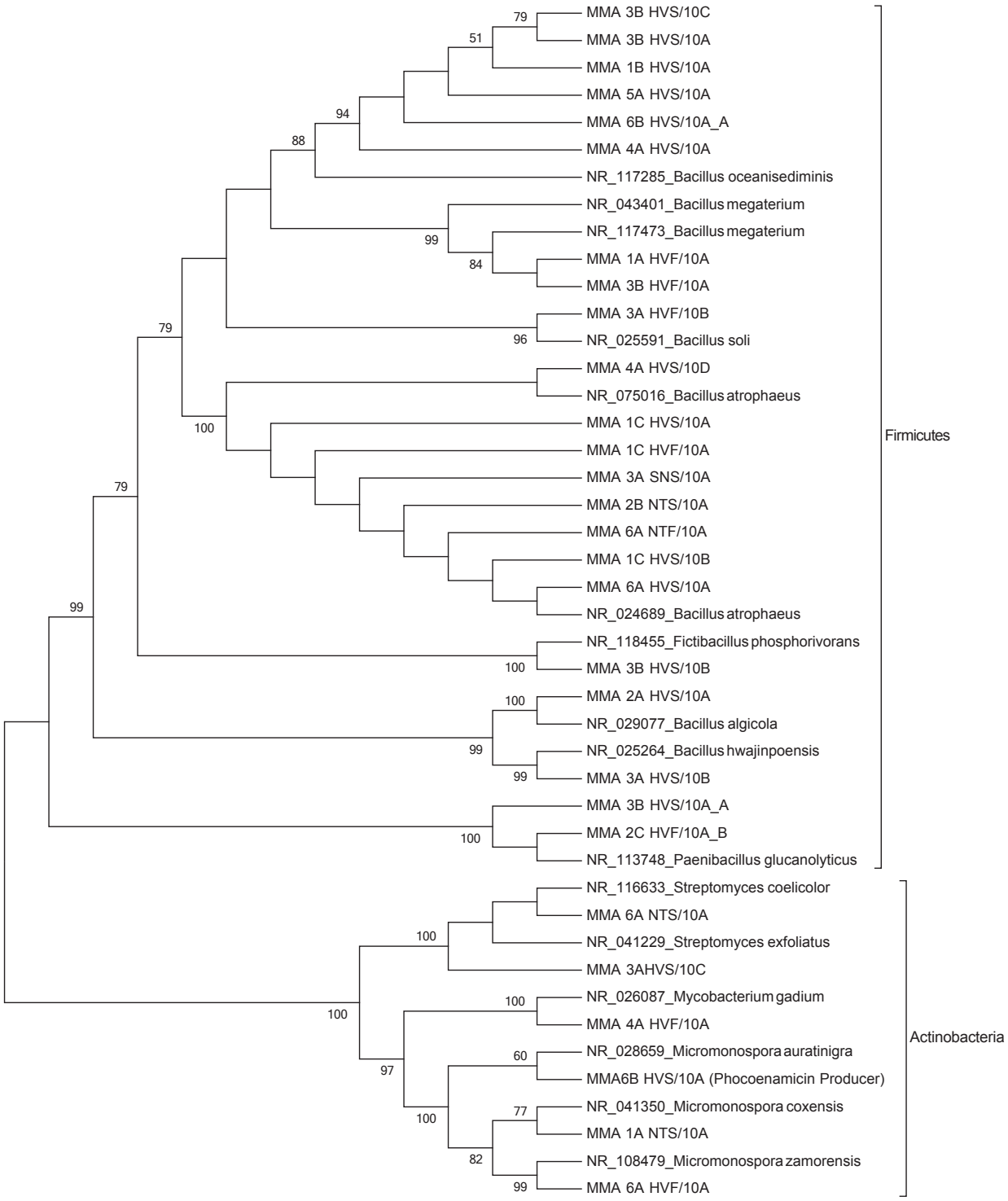

**Fig. S2. Molecular networking of bacterial extracts.** Colored nodes are metabolites produced only by one organism, nodes represented in grey are metabolites produced by many organisms.

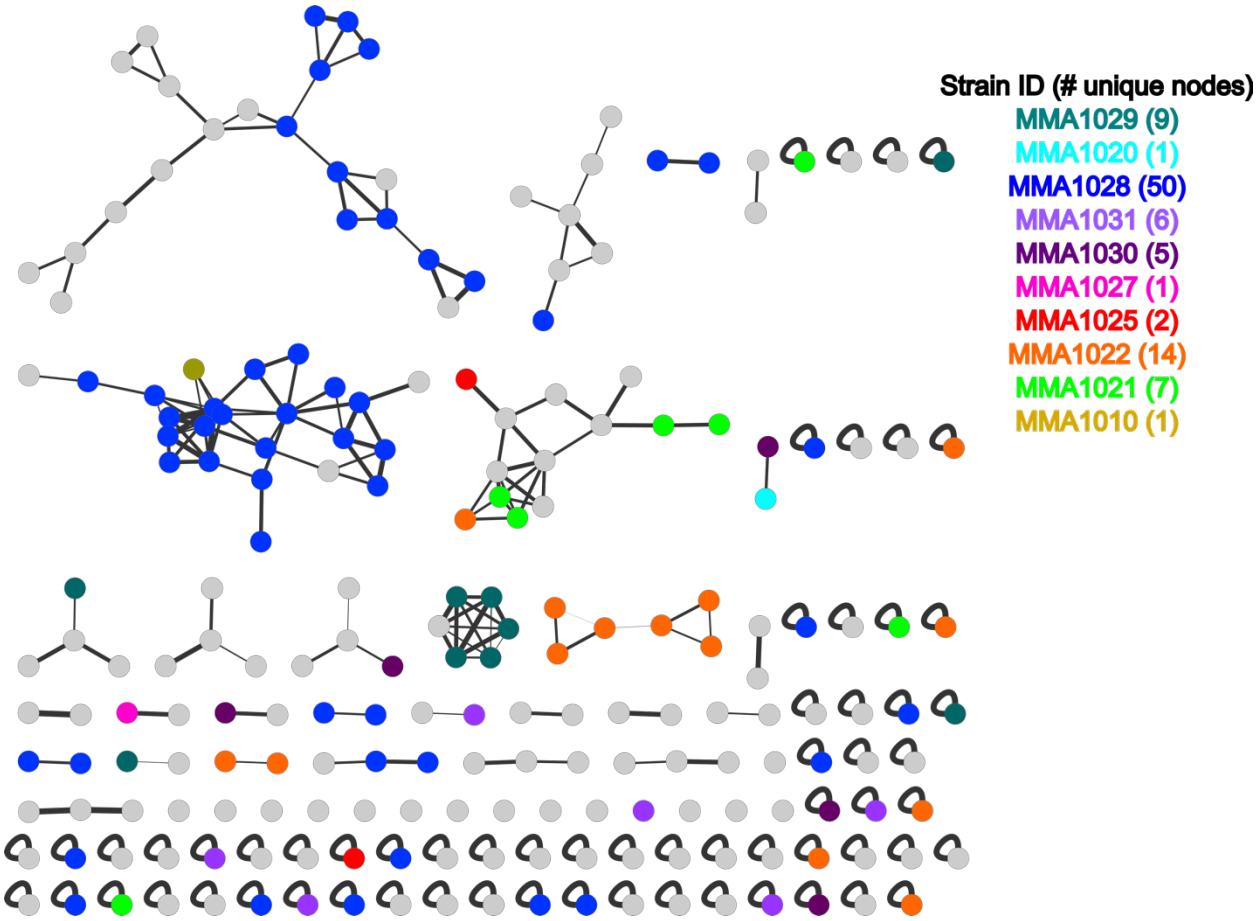

**Fig. S3. Structure elucidation of phocoenamicin.** (i) Key NMR correlations for subunits A (carbohydrates), B (aliphatic core), and C (cyclohexene unit). (ii) Key ROESY correlations for configurational analysis. (iii) HMBC correlations.

**i. Subunits**

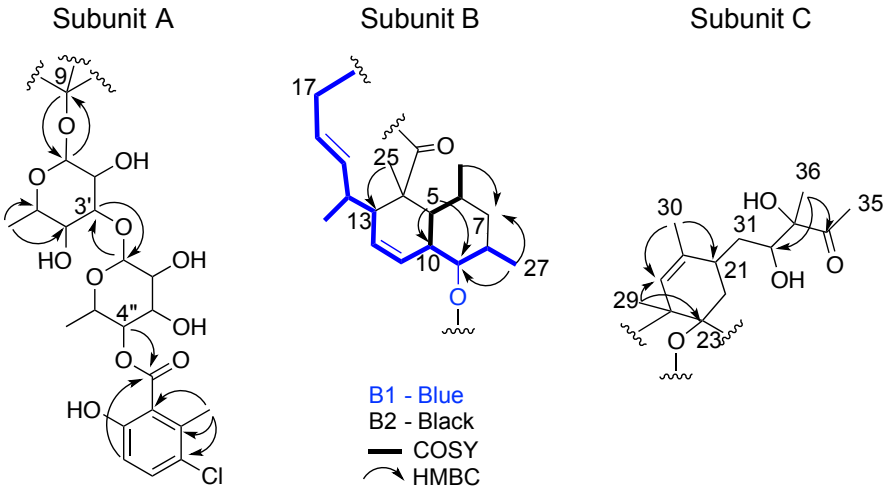


**ii. ROESY Correlations**

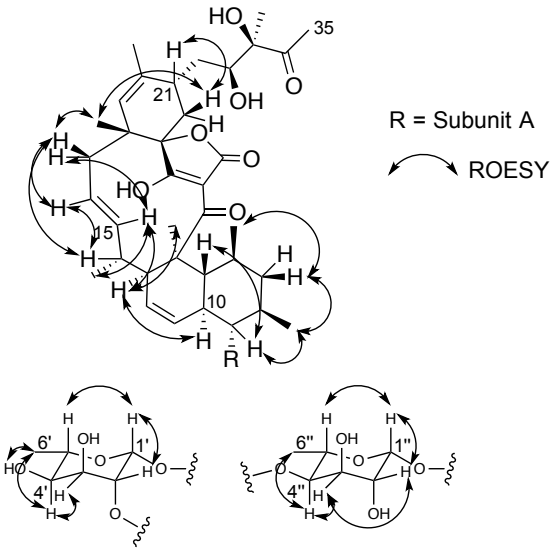


**iii. HMBC Correlations**

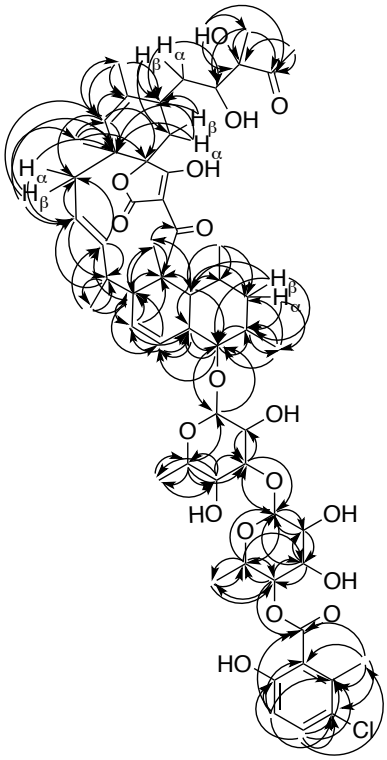

**Fig. S4. ROE correlations of possible diastereomers.** A combination of coupling constants and key ROE correlations indicated a configuration of 32S, 33R for the sidechain. To further justify this conclusion, all possible diastereomers of the side chain were modeled in Discovery Studio 4.0 (i, ii, iii). Except for the (32S, 33R) diastereomer shown in purple (iv), all other diastereomers were unable to reproduce all the observed ROE correlations. In any one confirmation, at least one observed ROE correlation was unobtainable in all the other models created. Examples of ROE correlations that were observed but not able to be replicated in the model without sacrificing other correlations are represented with yellow double headed arrows. Correlations in the models consistent with the observed data are displayed with white double-headed arrows.

i) SS Stereoisomer: Observed ROE correlation not reproducible in model in yellow

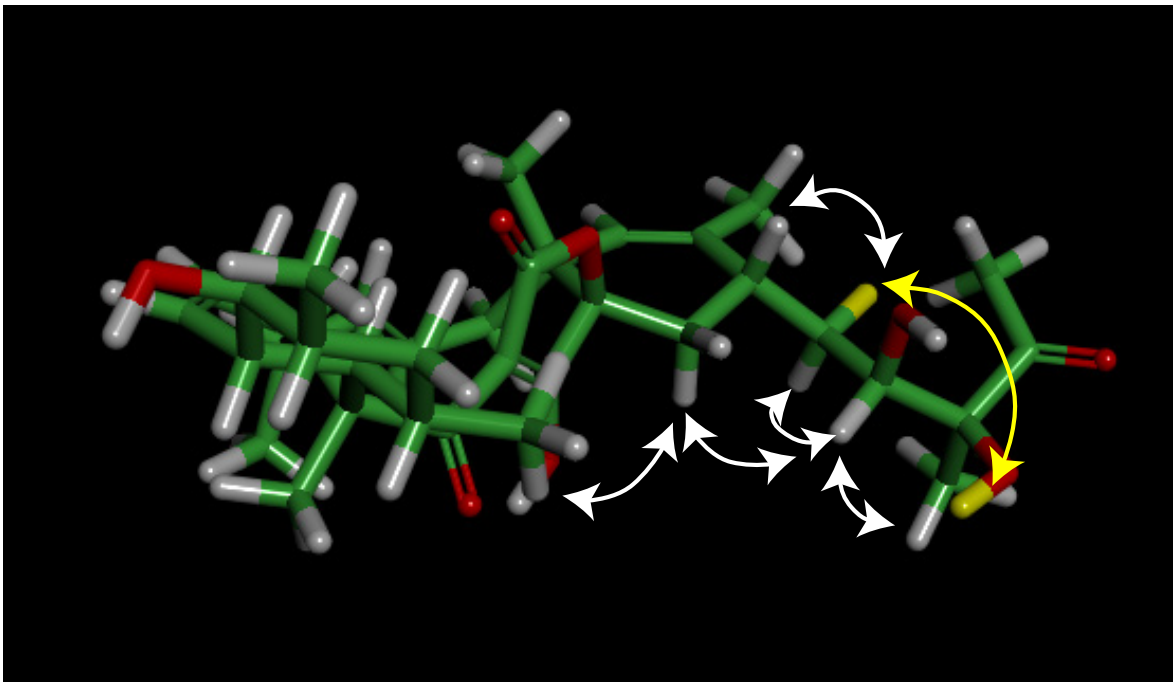

ii) SS Stereoisomer: Observed ROE correlation not reproducible in model in yellow

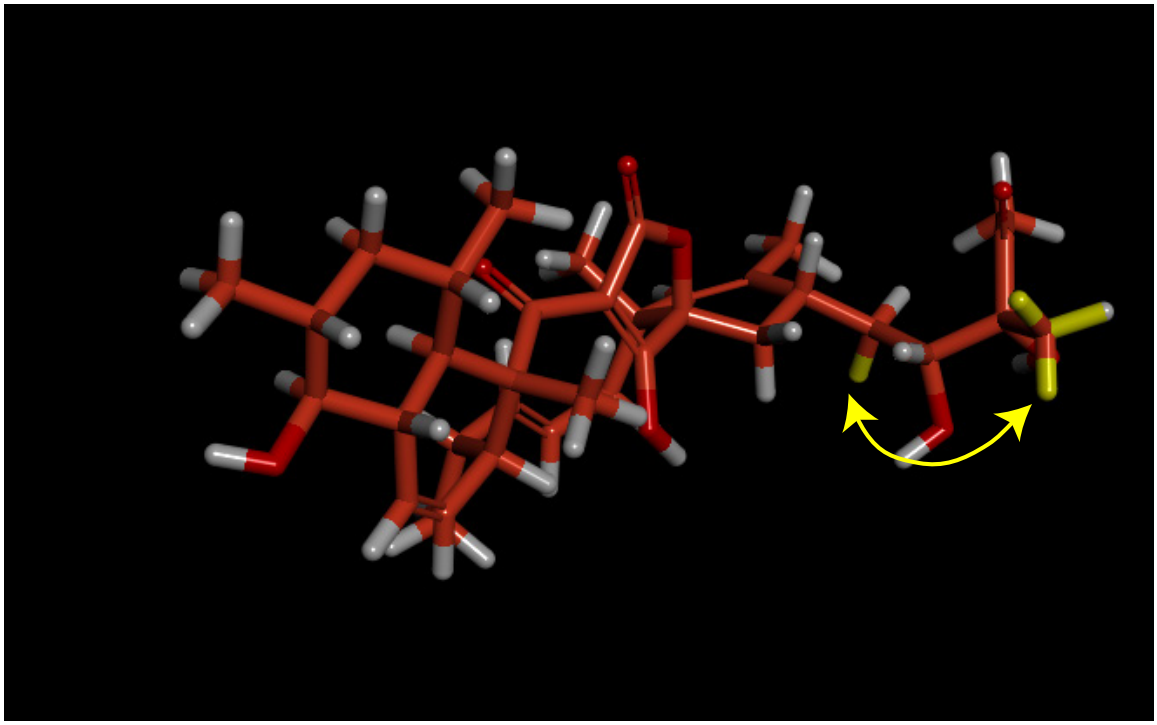

iii) RS Stereoisomer: Observed ROE correlation not reproducible in model in yellow

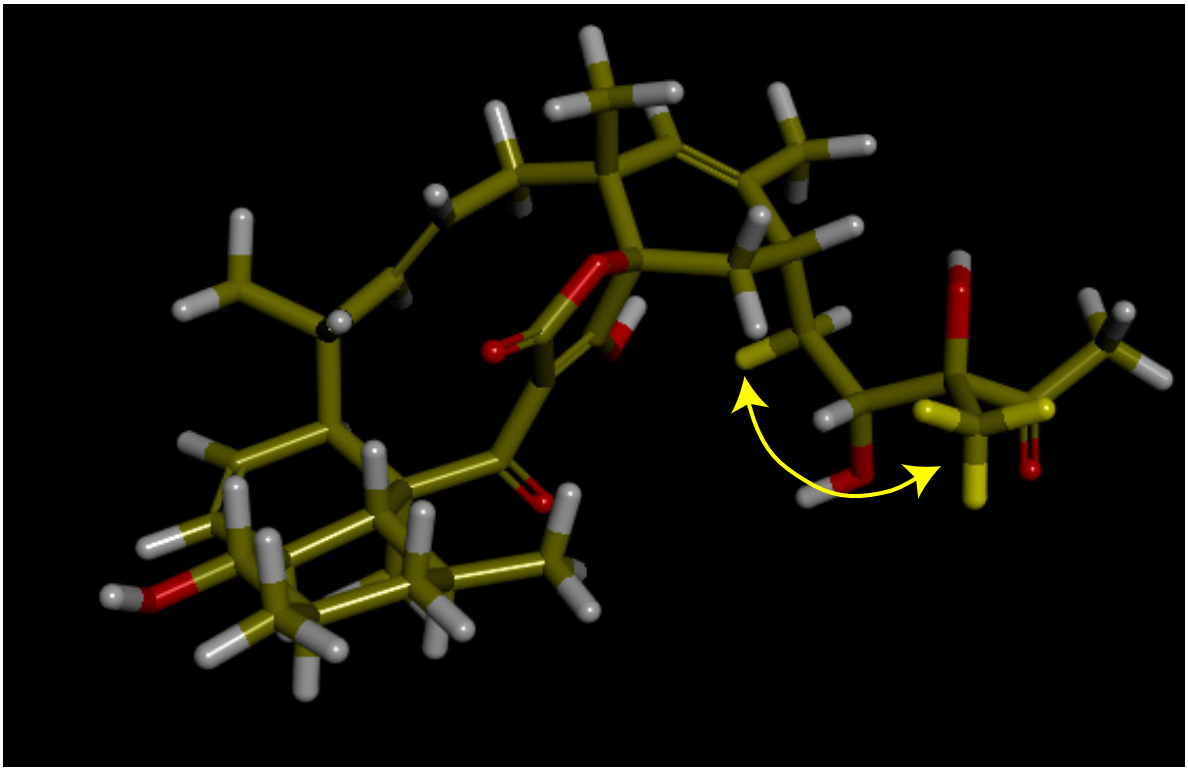

iv) SR: Matching NOE correlations to observed data in white

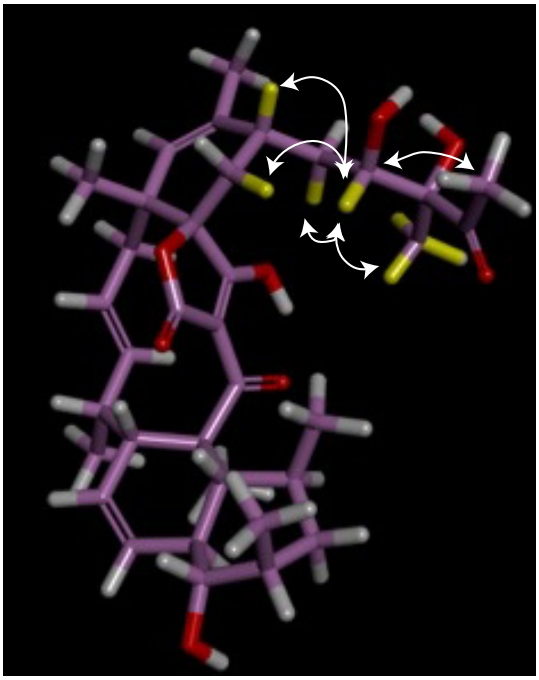

ROE correlations for proton on C32

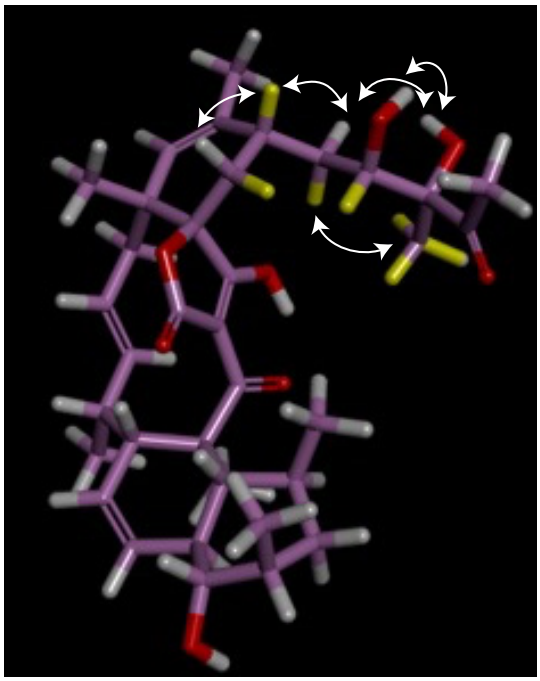

All other observed ROE correlations

**Fig. S5. LCMS trace of crude extract, RLFI1036F.** Spectra obtained using a gradient of MeCN:H2O + 0.02% formic acid (65% MeCN for 2 min, 65%-95% MeCN over 12 min) at a flow rate of 2 ml/min (Phenomenex Synergi Fusion-RP, 10 x 250 mm column)**.**

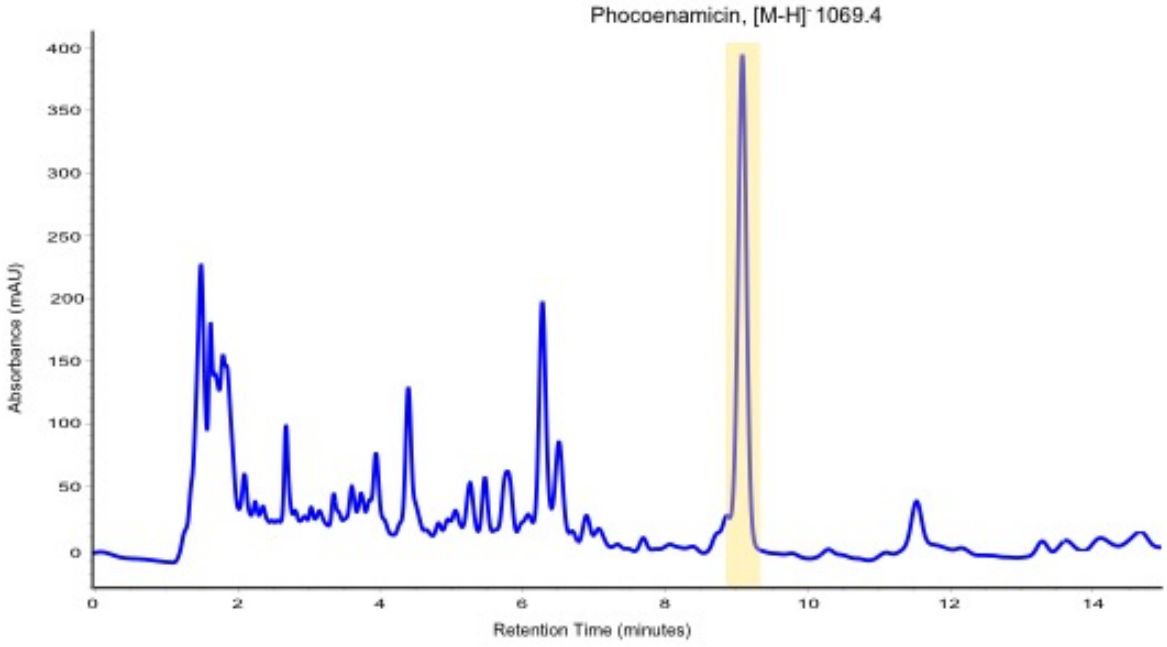

**Fig. S6A. $^{1}$H of phocoenamicin at 600 MHz in acetone-d6.**

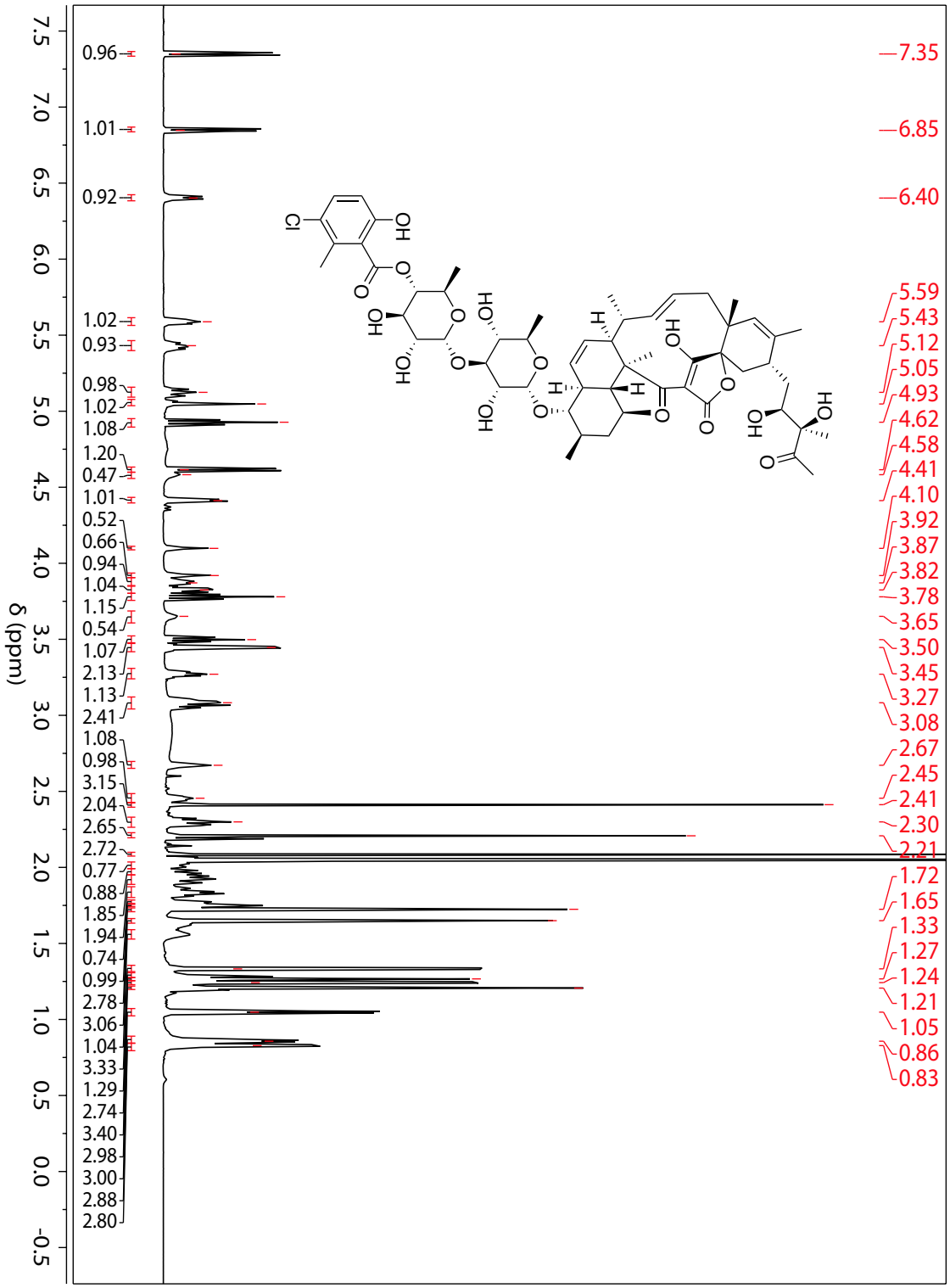

**Fig. S6B. gCOSY of phocoenamicin at 600 MHz in acetone-d6.**

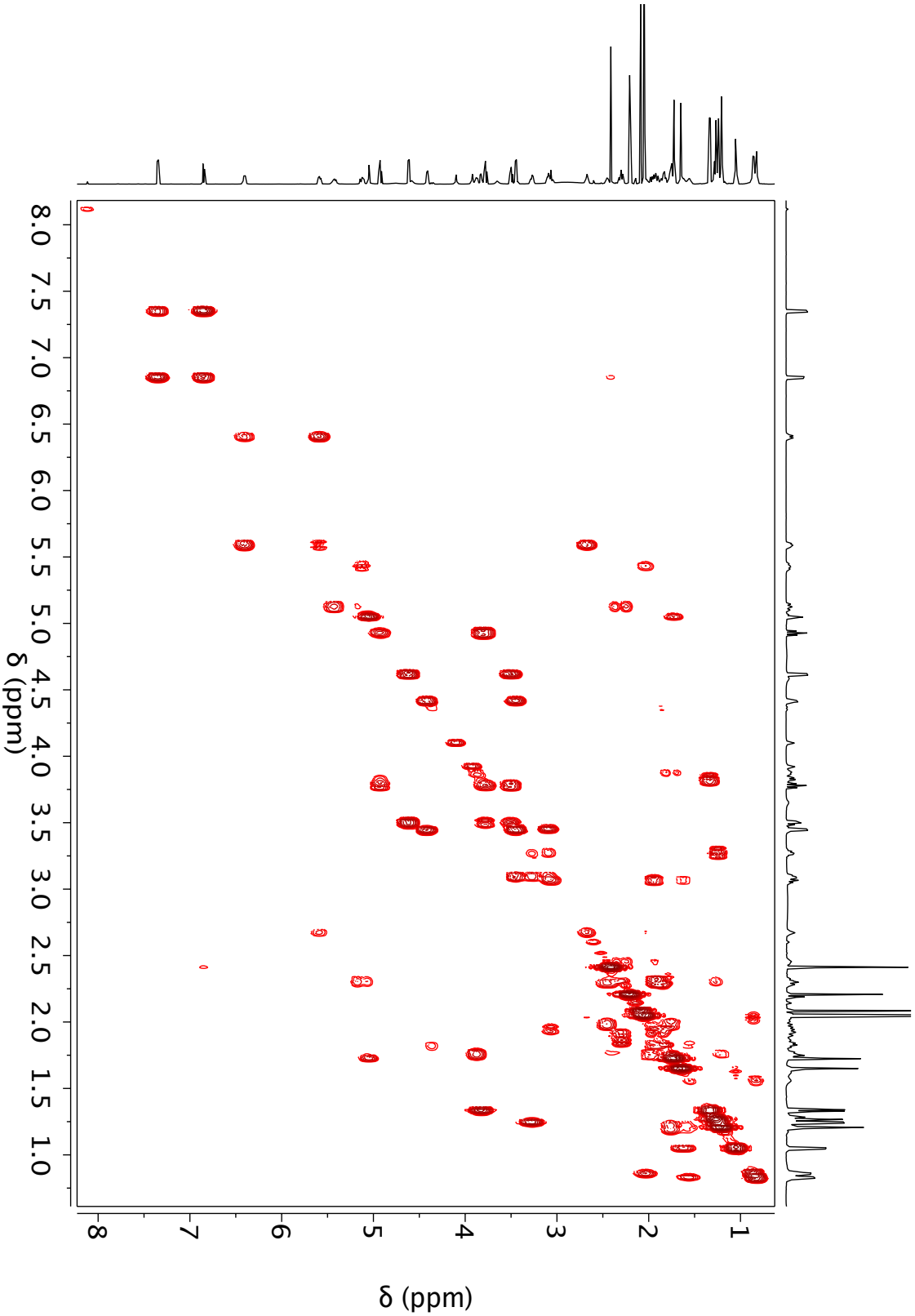

**Fig. S6C. gTOCSY of phocoenamicin at 600 MHz in acetone-d6.**

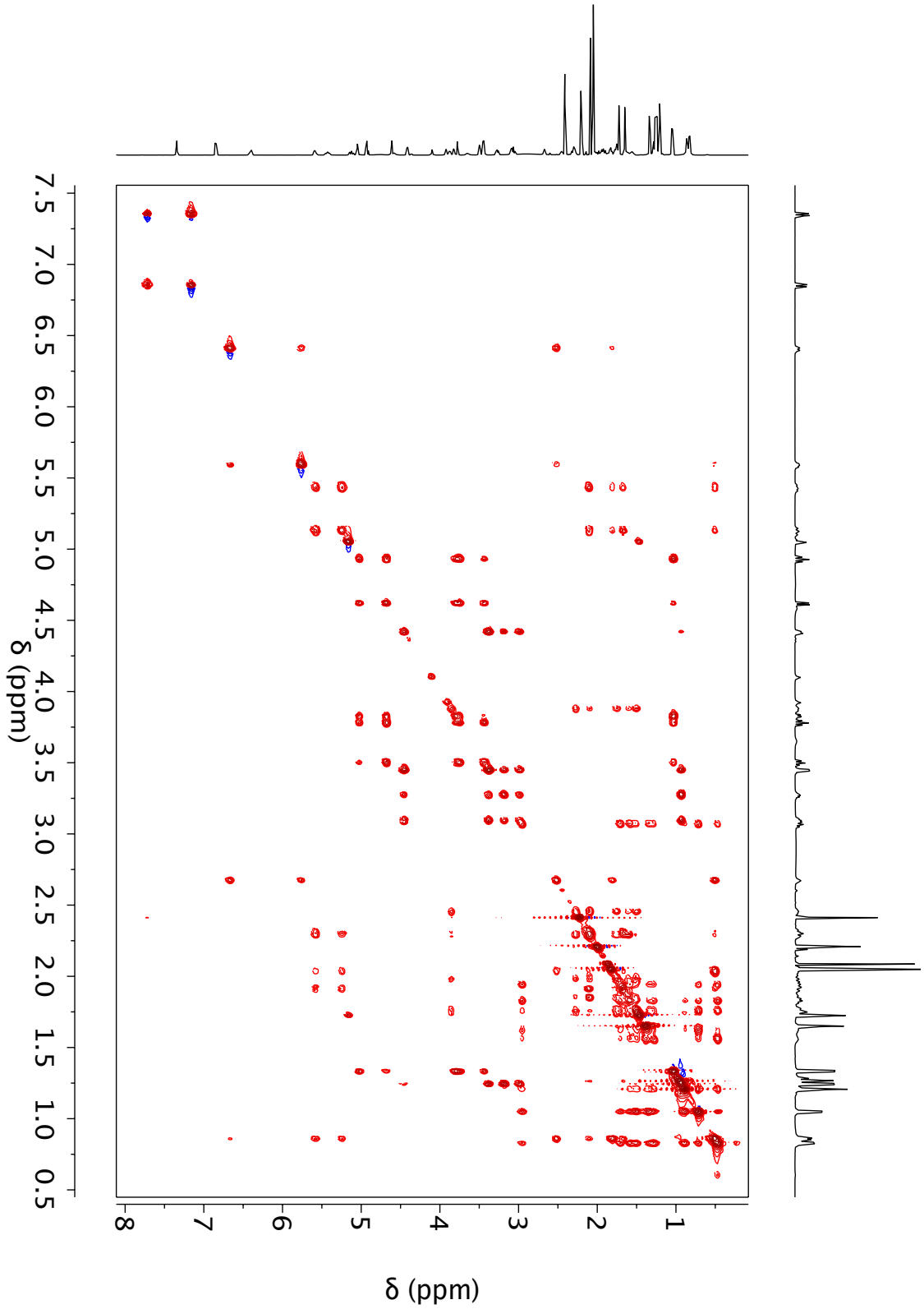

**Fig. S6D. HSQC of phocoenamicin at 600 MHz in acetone-d6.**

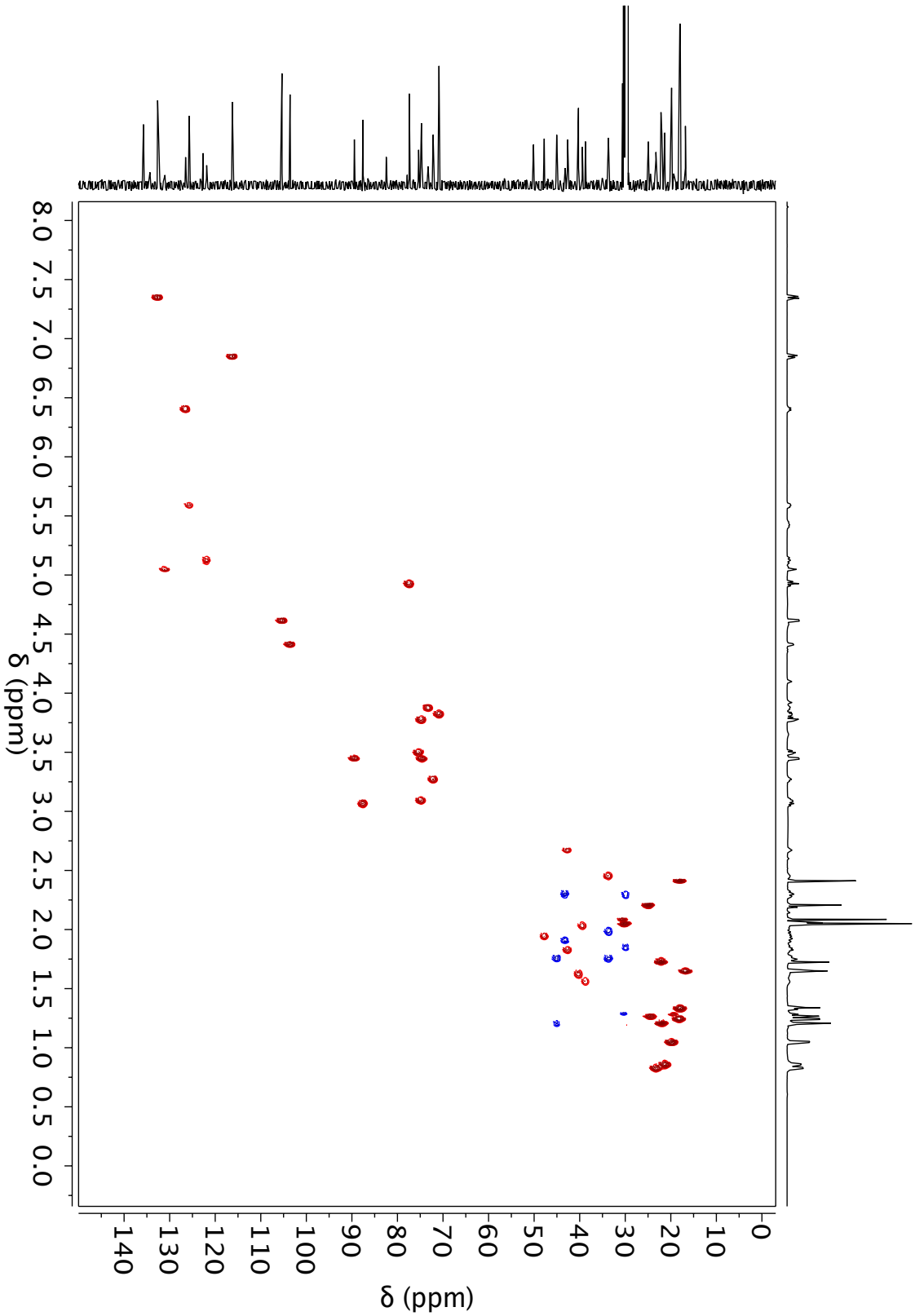

**Fig. S6E. HMBC of phocoenamicin at 600 MHz in acetone-d6.**

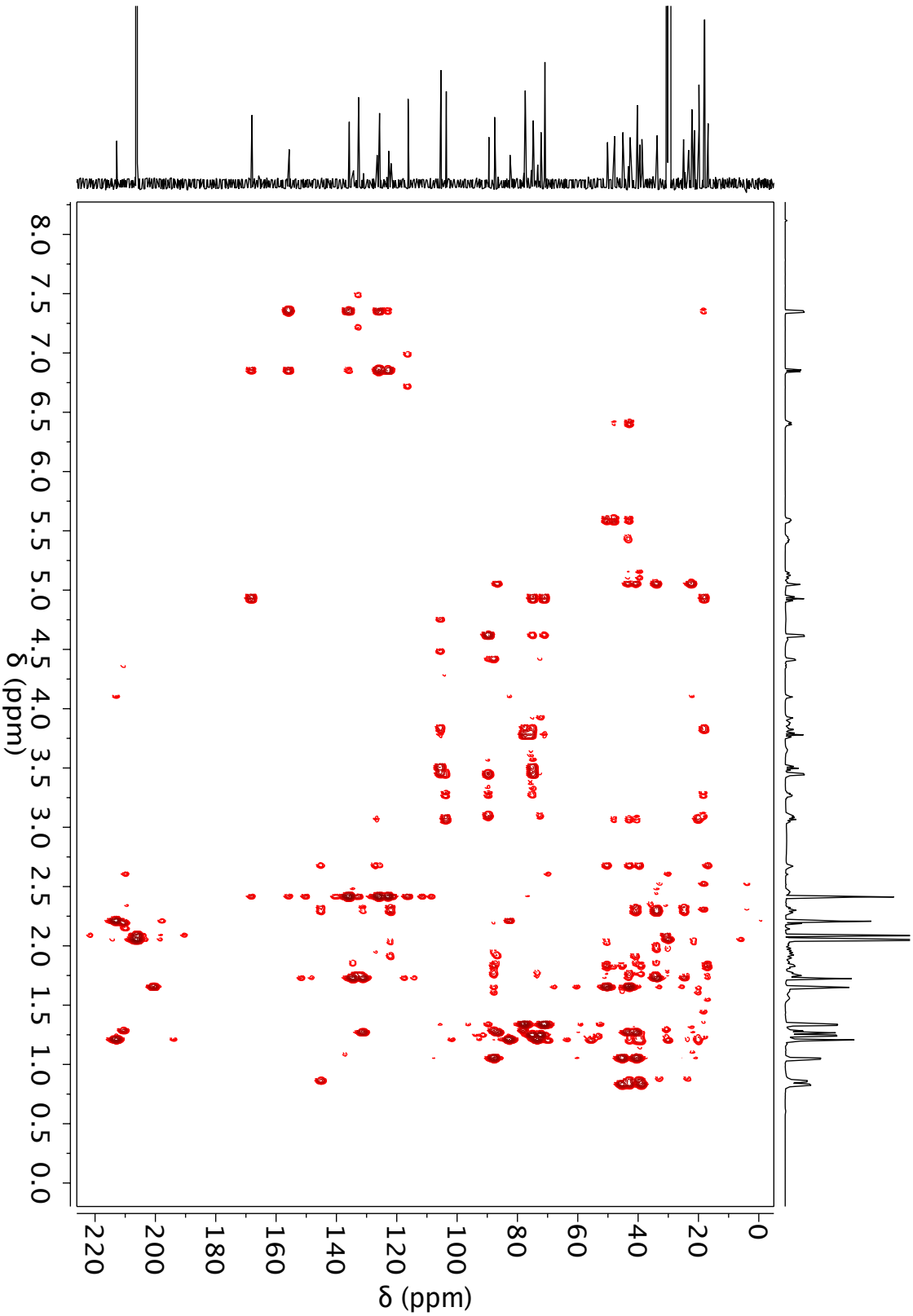

**Fig. S6F. ROESY of phocoenamicin at 600 MHz in acetone-d6.**

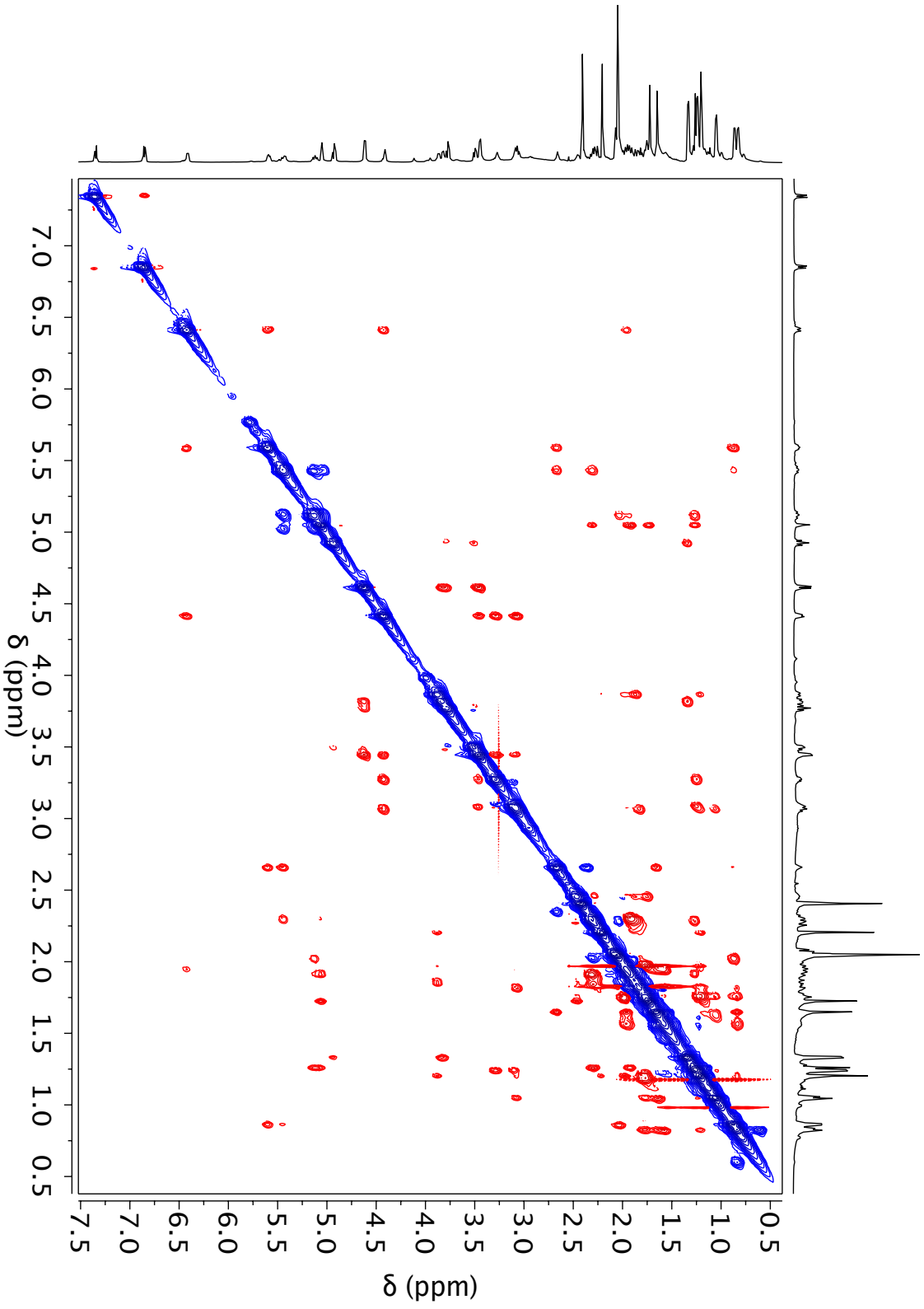

**Fig. S6G. $^{13}C$ of phocoenamicin at 600 MHz in acetone-d6.**

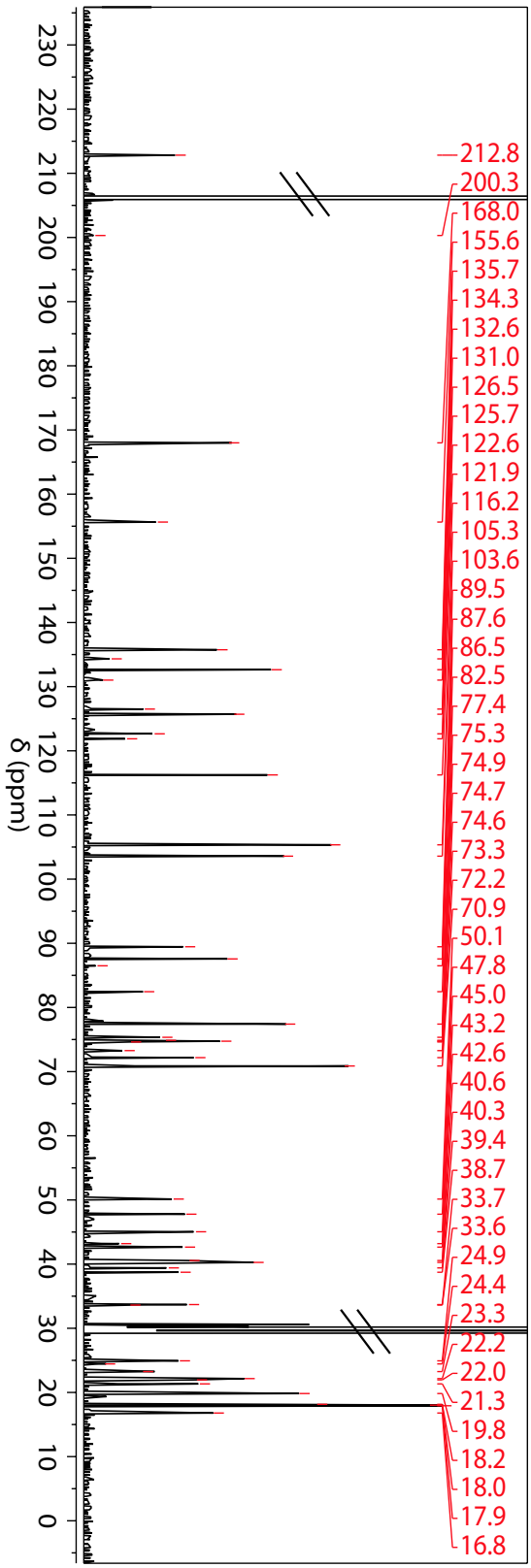

**Fig. S6H. 1D-TOCSY of phocoenamicin at 600 MHz in acetone-d6, irradiated at 2.45 ppm.**

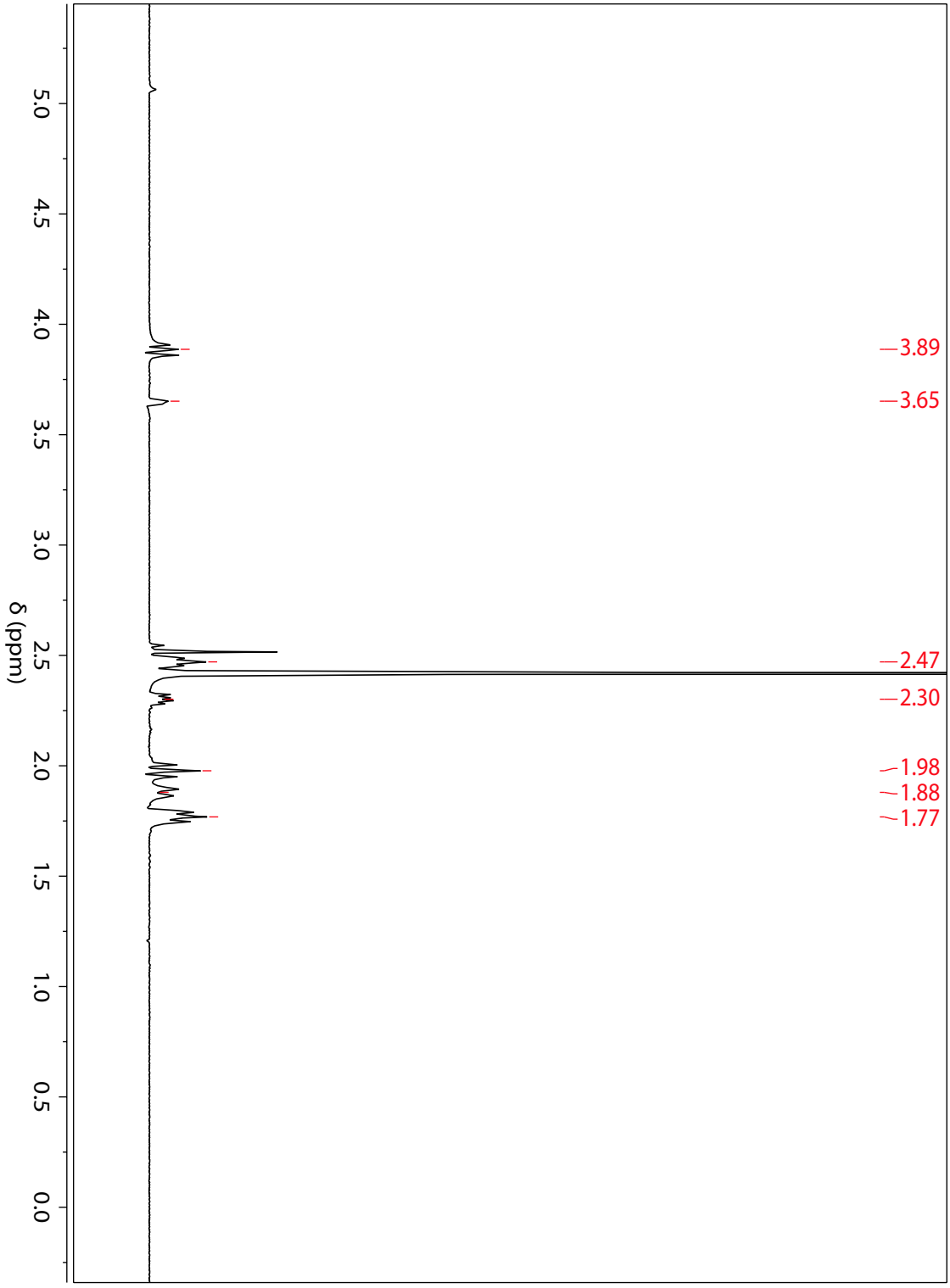

**Fig. S6I. 1D-TOCSY of phocoenamicin at 600 MHz in acetone-d6 irradiated at 5.1 ppm.**

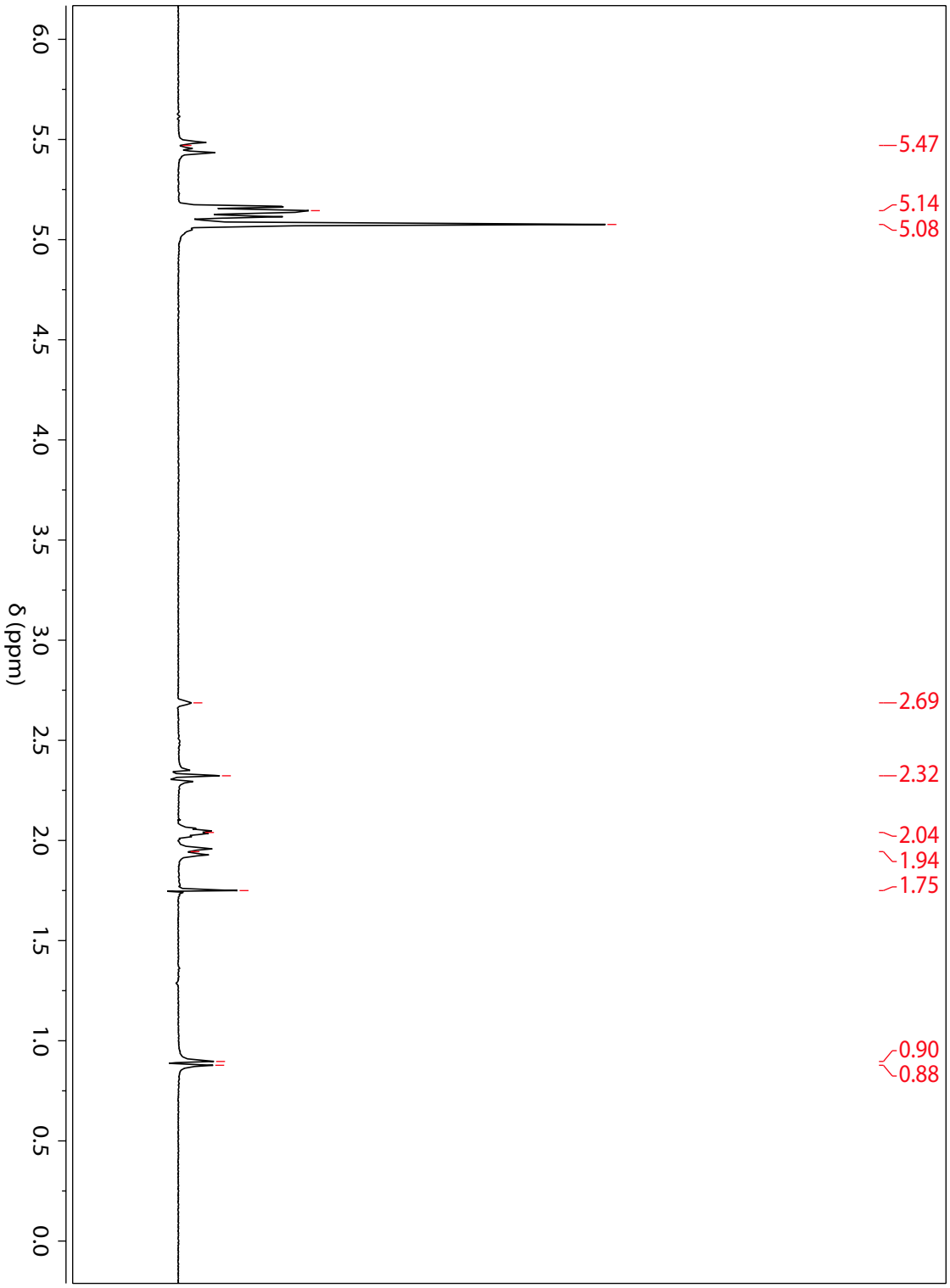

**Fig. S7. $^{1}$H of synthetic and isolated sugars at 600 MHz in chloroform-d1.**

Isolated triacetate 6-deoxy- β-D-glucopyranose

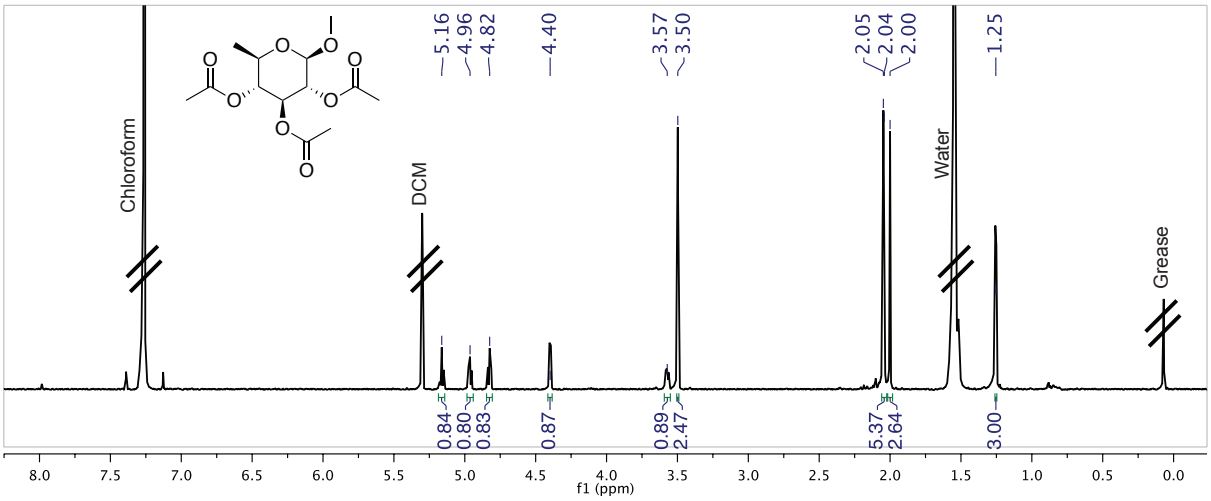


Synthetic triacetate 6-deoxy- β-D-glucopyranose

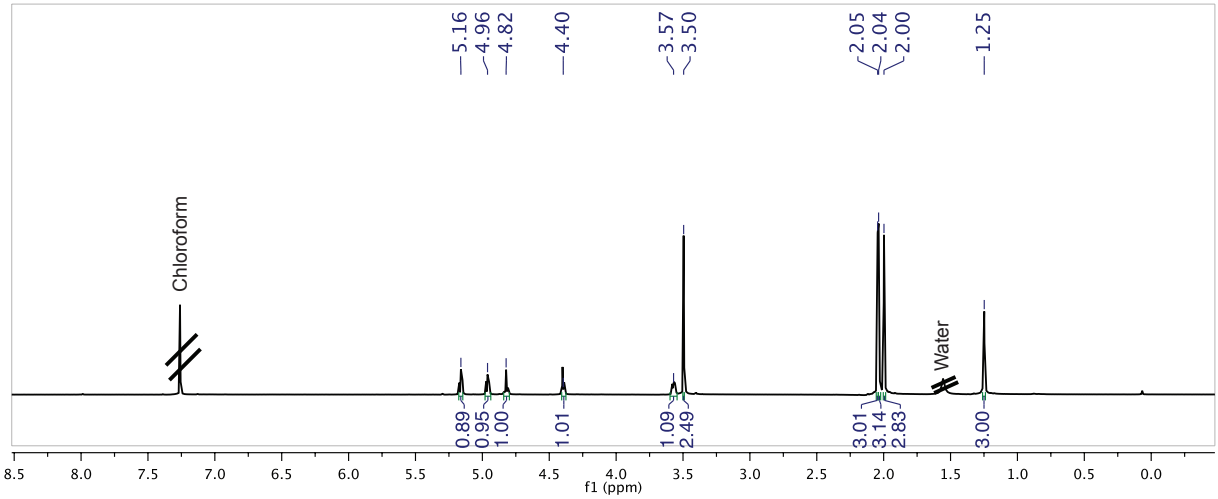

**Fig. S8. Synthetic and isolated sugar co-injection data.**

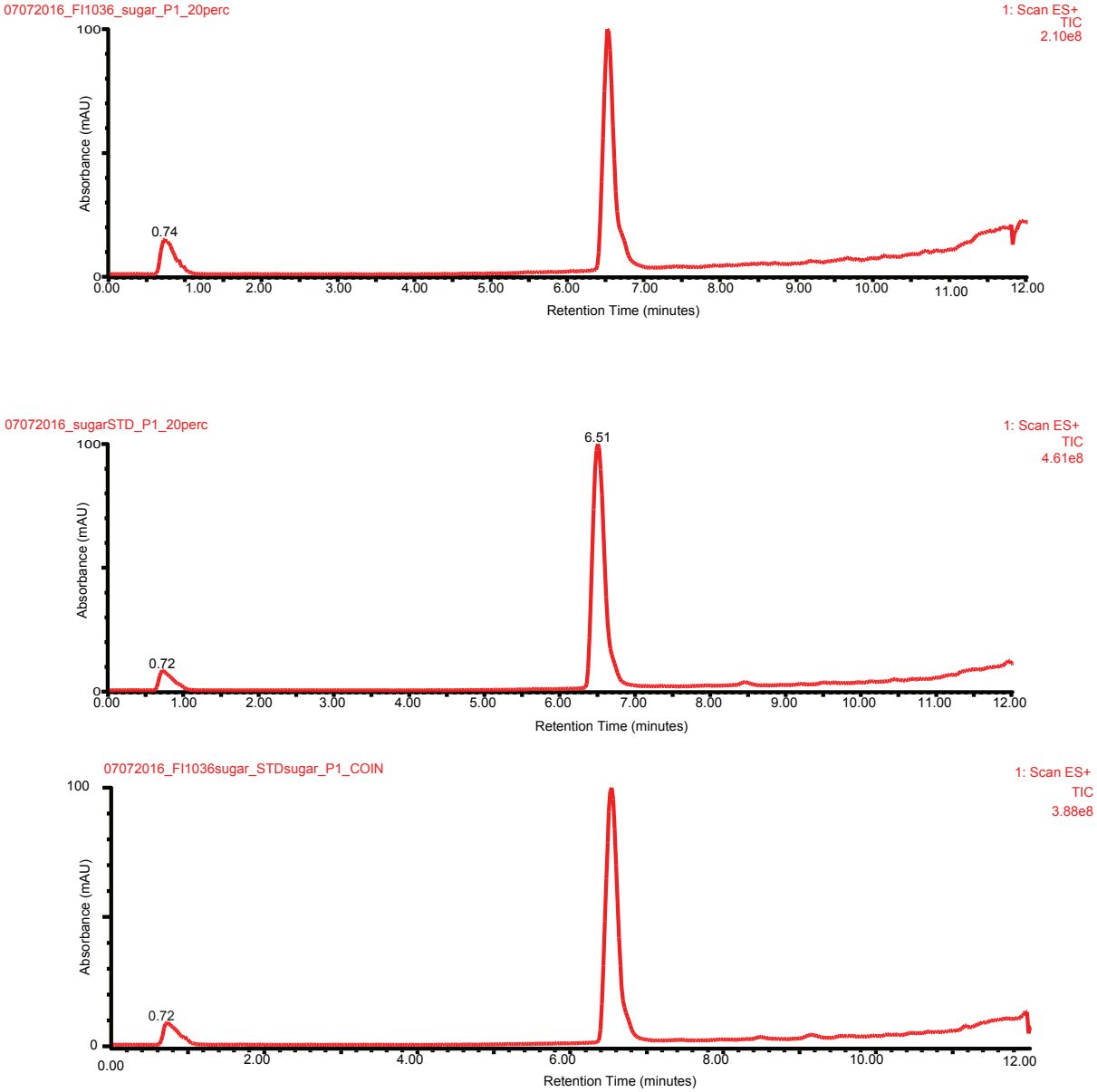

**Fig. S9. Cytological profiling data.** (A) Images of drug-treated HeLa cells stained with Hoechst dye (DNA), anti-phosphohistone H3 antibody (mitotic marker), and EDU (a clickable version of BrdU, a metabolically incorporated nucleoside analog used as an S-phase marker). Cells undergoing DNA synthesis are green, mitotic cells are pink, and cell nuclei are blue. (B) Color bar used to generate cytological profiling fingerprints in Fig. 5

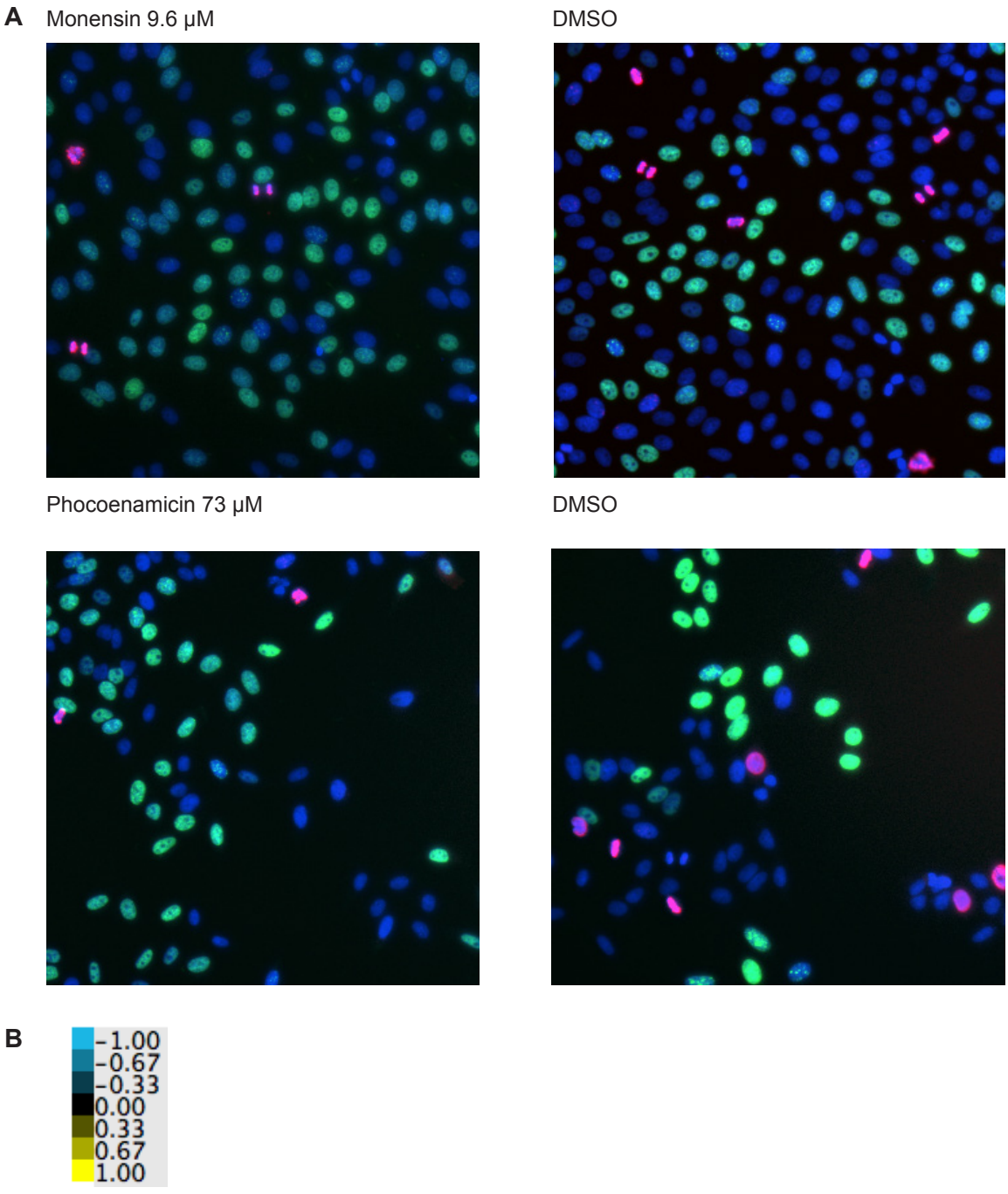

**Fig. S10. Flow cytometry of *S. aureus* cells treated with phocoenamicin.** Results were acquired in triplicate for cells incubated with the membrane potential dye ($DiOC_2$) and treated with CCCP or various concentrations of phocoenamicin around the MIC. Vertical axis represents cell count and is staggered by compound-treatment condition. Average red:green fluorescence ratio represented in bar graph, with error bars representing standard deviation across the triplicate runs.

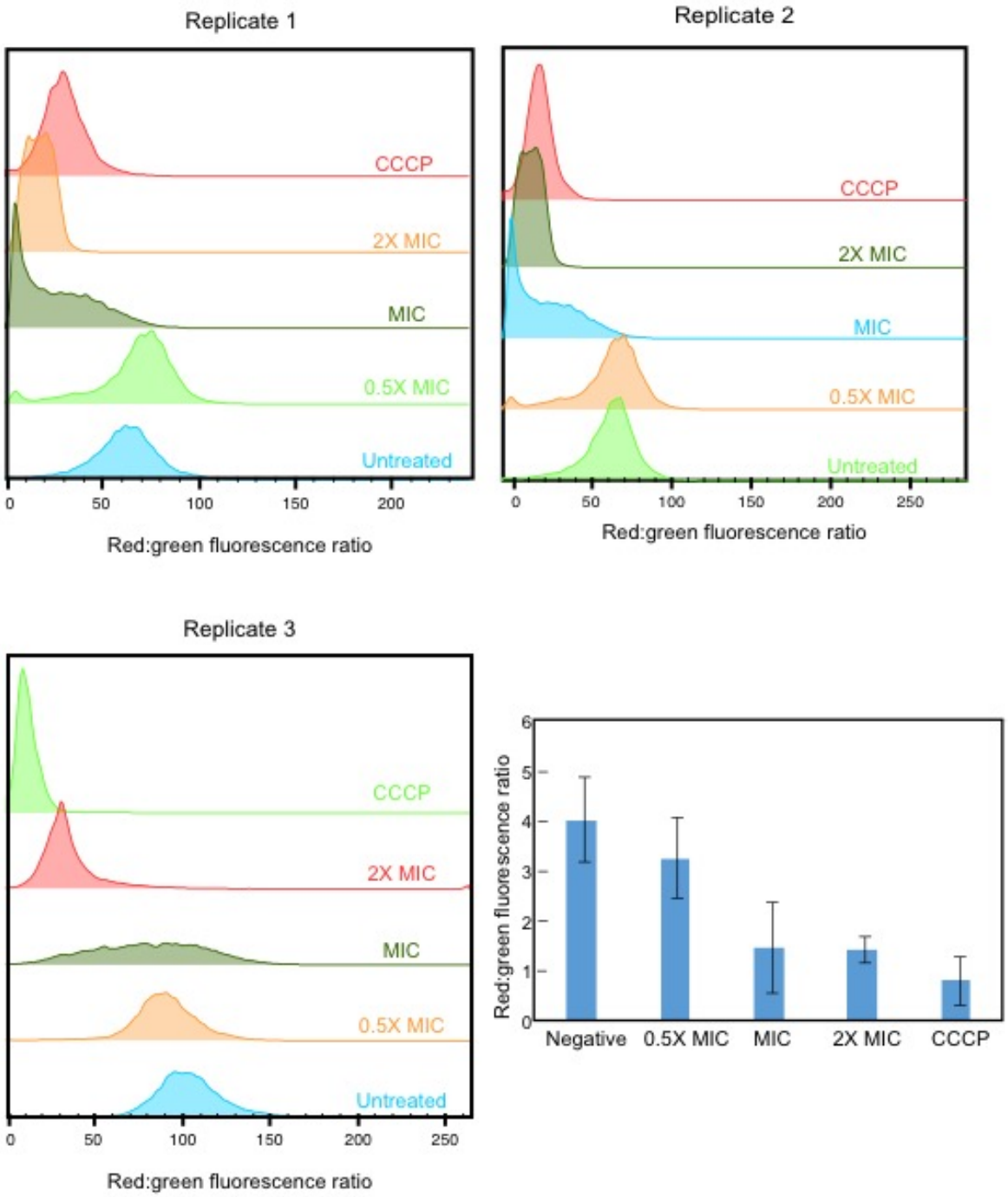

**Fig. S11. Genetic screen attempting to identify the cellular target of phocoenamicin.** (A) Screen of *Bacillus subtilis* essential gene knockdown library against phocoenamicin. Relative fitness distribution of CRISPRi knockdown strains grown on plates containing sub-inhibitory concentrations of trimethoprim (left) and phocoenamicin (right). Screens were performed and relative fitness determined as in previous protocols (38). Strains sensitized to the antibiotic by depletion of the essential gene target are expected to have a lower relative fitness. The target of trimethoprim was accurately identified as DfrA. By contrast, no apparent target was observed for phocoenamicin. (B) Identification of transposon-insertion sites of the strains showing resistance to phocoenamicin. *B. subtilis* transposon insertion library was plated on LB agar plates containing 4X MIC of phocoenamicin. After 16 h incubation, 95 phocoenamicin-resistant colonies were isolated and the transposon-insertion site was mapped for 20 strains. All 20 transposon insertions were located upstream of the *mdtR-mdtP* operon, inducing overexpression of *mdtP*, which encodes a multidrug efflux pump. Inserted positions (red line) were labeled with coordinates and isolate number (in parentheses).

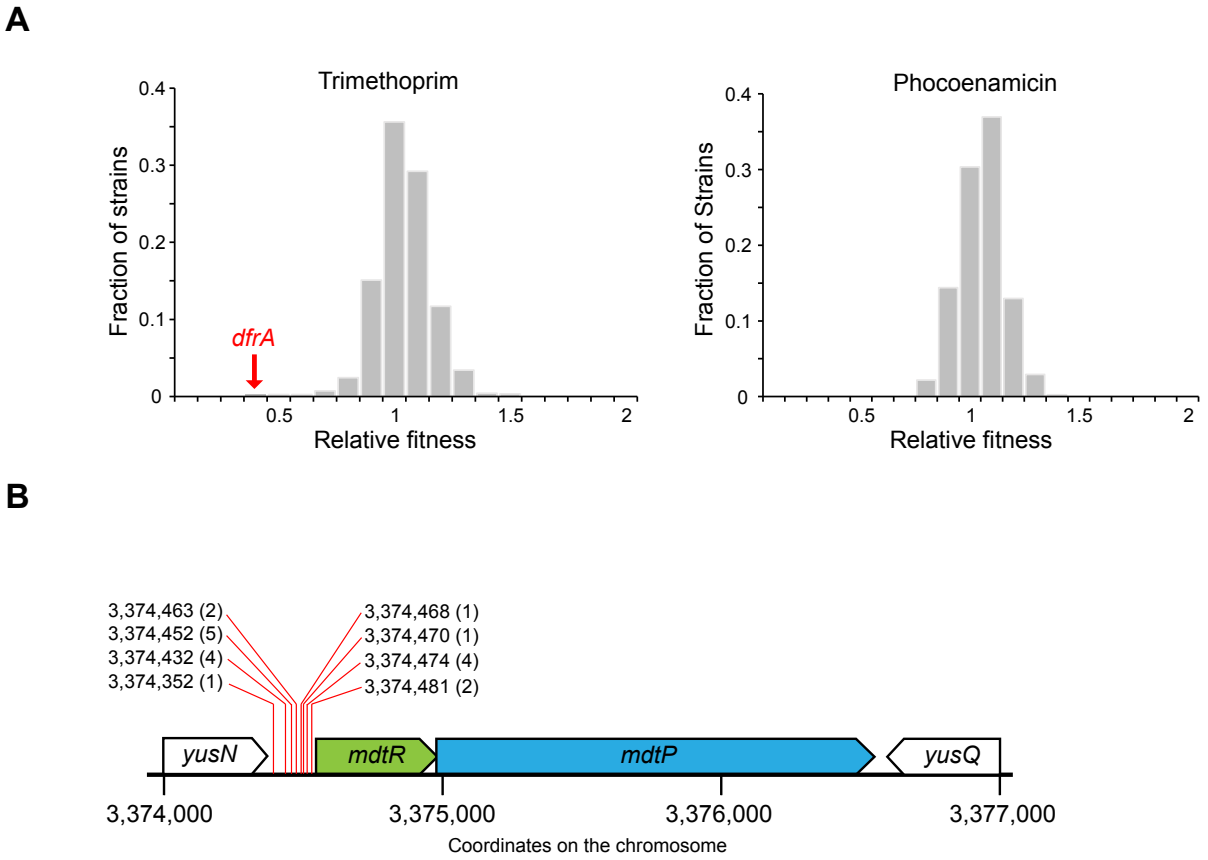

**Fig. S12. Propidium iodide (PI) staining shows that phocoenamicin does not permeabilize the cell membrane of *S. aureus* cells.** Cells were grown overnight in MB medium, back-diluted 1:100 in fresh MB, and then incubated in CellASIC microfluidic chips with the ONIX perfusion system at 37 °C while imaging. 75 μM PI was added to the perfusion medium and cells were treated with DMSO, 0.5X MIC phocoenamicin, or 75% ethanol. The amount of DMSO added was equivalent to volume present in 0.5X MIC phocoenamicin. For ethanol, cells were treated in an Eppendorf tube, spun down, and then washed in medium before transfer to the CellASIC chip (to avoid ethanol disruption of the fluidics system). (A) Representative images of PI fluorescence in each treatment. Time is measured relative to the time treatment began. Only ethanol treatment causes PI staining. (B) Cell outlines were detected using *Morphometrics*.[5] Average PI fluorescence increases a few minutes after ethanol treatment, whereas fluorescence remains approximately constant after phocoenamicin and DMSO treatment. Error bars are standard deviation over $n > 150$ cells for each treatment.

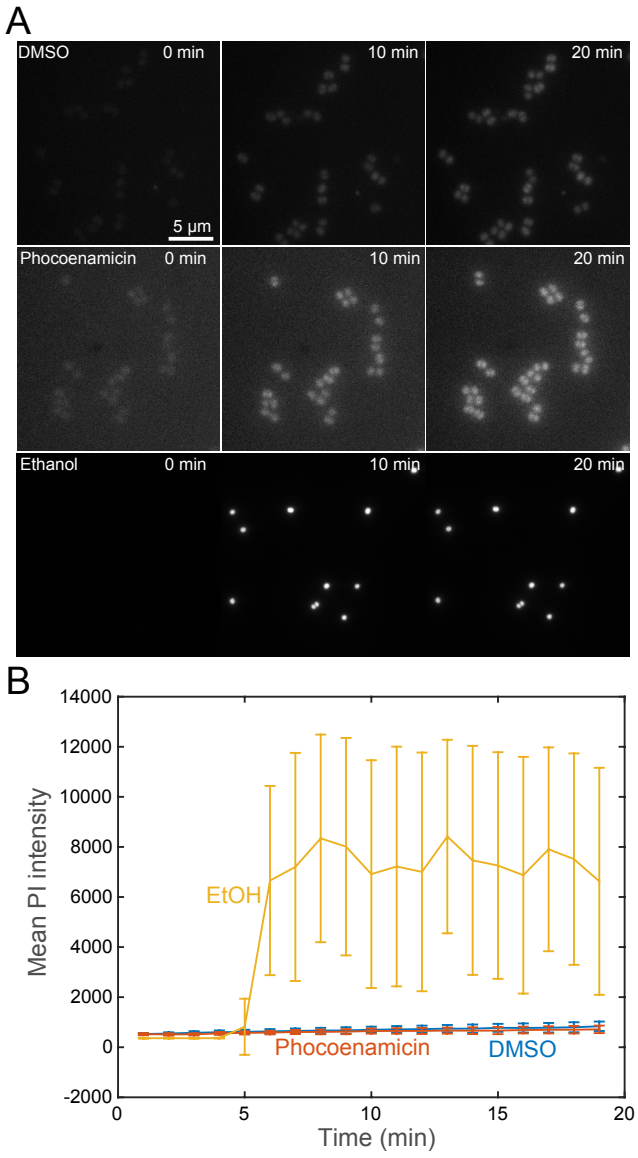

**Table S1. Marine mammal necroscopy details.** Whole dead intact mammals were recovered as part of the California Marine Mammal Stranding Network, and stored at -20 °C until dissection. All instruments were flame sterilized prior to dissection and after each cut. The stomach and gastrointestinal tract were separated from the body cavity. 1 mL aliquots sampled along the digestive tract were transferred to sterile 10-mL Falcon tubes at discrete regions: the posterior portion of the intestine, the mid-intestine, the stomach, and the duodenum, as appropriate for each specimen.

| Code | Specimen | Species | Common name | Details |
|---|---|---|---|---|
| MMA | LMLPP2011SEP29 | *Phocoena phocoena* | Harbor porpoise | Adult female, killed by dolphins |
| MMB | LMLPV2013MAR03 | *Phoca vitulina* | Harbor Seal | Adult female, possible infection |
| MMC | LMLZC2013APR10 | *Zalophus californianus* | California Sea Lion | Adult female, emaciated |
| MMD | LMLPP2013JUL23 | *Phocoena phocoena* | Harbor porpoise | Infant, killed by dolphins |
| MME | LMLDC2013JUL31 | *Dolphinus capensis* | Common dolphin | Infant, death by separation |

**Table S2. 16S Sequencing data and organism nomenclature.** % identity represents the sequence identity to the closest published strain in NCBI. All extracts are given MMAXX identification codes, only extracts prioritized for biological assays were given RLFI_XXXX codes.

| Organism name | MMA10XX | RLFI_XXXX | Accession number | Closest NCBI strain accession number | Description | % identity |
|---|---|---|---|---|---|---|
| MMA 2A HVS/10A | MMA1001 | RLFI_1034 | KY580789 | NR_029077.1 | *Bacillus algicola* | 98.6 |
| MMA 1B HVS/10A | MMA1002 | NA | KY580790 | NR_025842.1 | *Bacillus firmus* | 99.9 |
| MMA 3A HVF/10B | MMA1006 | NA | KY580791 | NR 025591.1 | *Bacillus soli* strain R-16300 | 98.6 |
| MMA 3A HVS/10C | MMA1009 | NA | KY580792 | NR_116633.1 | *Streptomyces coelicolor* strain DSM | 100.0 |
| MMA 3A HVS/10B | MMA1010 | RLFI_1038 | KY580793 | NR_025264.1 | *Bacillus hwajinpoensis* strain SW-72 | 100.0 |
| MMA 4A HVS/10A | MMA1011 | NA | KY580794 | NR_117285.1 | *Bacillus oceanisediminis* strain H2 | 99.6 |
| MMA 6B HVS/10A_A | MMA1012 | NA | KY580795 | NR_025842.1 | *Bacillus firmus* strain IAM 12464 | 98.8 |
| MMA 1C HVS/10A | MMA1013 | NA | KY580796 | NR_024689.1 | *Bacillus atrophaeus* | 99.8 |
| MMA 1C HVF/10A | MMA1014 | NA | KY580797 | NR_024689.1 | *Bacillus atrophaeus* | 99.9 |
| MMA 6A HVF/10A | MMA1017 | RLFI_1043 | KY580798 | NR_108479.1 | *Micromonospora zamorensis* | 99.5 |
| MMA 4A HVF/10A | MMA1019 | RLFI_1044 | KY580799 | NR_026087.1 | *Mycobacterium gadium* strain 1066 | 99.3 |
| MMA 1A HVF/10A | MMA1020 | NA | KY580800 | NR_043401.1 | *Bacillus megaterium* strain IAM 13418 | 99.6 |
| MMA 3B HVF/10A | MMA1021 | RLFI_1039 | KY580801 | NR_117473.1 | *Bacillus megaterium* strain ATCC 14581 | 99.9 |
| MMA 5A HVS/10A | MMA1023 | NA | KY580802 | NR_117285.1 | *Bacillus oceanisediminis* strain H2 | 99.6 |
| MMA 3B HVS/10C | MMA1024 | NA | KY580803 | NR_117285.1 | *Bacillus oceanisediminis* strain H2 | 98.4 |
| MMA 2B HVS/10A | MMA1025 | NA | KY580804 | NR_117285.1 | *Bacillus oceanisediminis* strain H2 | 94.4 |
| MMA 3B HVS/10B | MMA1027 | RLFI_1040 | KY580805 | NR_118455.1 | *Fictibacillus phosphorivorans* | 99.5 |
| MMA 6A NTS/10A | MMA1028 | RLFI_1041 | NA | NA | NA | NA |
| MMA 6A NTS/10A | MMA1029 | RLFI_1042 | KY580806 | NR_041229.1 | *Streptomyces exfoliatus* strain NBRC 13475 | 100.0 |
| MMA 4A HVS/10D | MMA1033 | NA | KY580807 | NR_07016.1 | *Bacillus atrophaeus* strain 1942 | 99.8 |
| MMA 2C HVF/10A_B | MMA1035 | NA | KY580808 | NR_113748.1 | *Paenibacillus glucanolyticus* | 99.7 |
| MMA 1A NTS/10A | MMA1036 | RLFI_1035 | KY580809 | NR_041350.1 | *Micromonospora coxensis* | 98.8 |
| MMA 6B HVS/10A | MMA1037 | RLFI_1036 | KY580810 | NR_028659.1 | *Micromonospora auratinigra* strain TT1-11 | 99.0 |
| MMA 3B HVS/10A_A | MMA1039 | RLFI_1037 | KY580811 | NR_113748.1 | *Paenibacillus glucanolyticus* strain NBRC 15330 | 99.8 |
| MMA 2A SNS/10A | MMA1041 | NA | KY580812 | NR_075016.1 | *Bacillus atrophaeus* strain 1942 | 99.9 |
| MMA 2B NTS/10A | MMA1042 | NA | KY580813 | NR_075016.1 | *Bacillus atrophaeus* strain 1942 | 99.9 |
| MMA 6A HTF/10A | MMA1043 | NA | KY580814 | NR_075016.1 | *Bacillus atrophaeus* strain 1942 | 99.9 |
| MMA 1C HVS/10B | MMA1044 | NA | KY580815 | NR_075016.1 | *Bacillus atrophaeus* strain 1942 | 99.9 |
| MMA 6A HVS/10A | MMA1045 | NA | KY580816 | NR_075016.1 | *Bacillus atrophaeus* strain 1942 | 99.9 |

**Table S3. NMR chemical shifts for phocoenamicin at 600 MHz in acetone-d6.**

| Position | $\delta_H$ (*J* in Hz) | $\delta_C$ |
|---|---|---|
| 1 | - | 175.0, qC |
| 2 | - | 106.9, qC |
| 3 | - | 200.3, qC |
| 4 | - | 50.1, qC |
| 5 | 1.82, m | 42.6, CH |
| 6 | 1.56, m | 38.7, CH |
| 7α | 1.75, m | 45.0, $CH_2$ |
| 7β | 1.20, m | - |
| 8 | 1.62, m | 40.3, CH |
| 9 | 3.07, dd (10.2, 10.2) | 87.6, CH |
| 10 | 1.94, 1.94, m | 47.8, CH |
| 11 | 6.40, d (10.0) | 126.5, CH |
| 12 | 5.59, ddd (10.0, 6.0, 2.4) | 125.5, CH |
| 13 | 2.67, m | 42.6, CH |
| 14 | 2.03, m | 39.4, CH |
| 15 | 5.43, dd (15.0, 9.0) | 144.7, CH |
| 16 | 5.12, ddd (15.9, 10.8, 2.4) | 121.9, CH |
| 17α | 2.30, dd (12.6, 10.8) | 43.2, $CH_2$ |
| 17β | 1.91, dd (12.6, 2.4) | - |
| 18 | - | 40.6, qC |
| 19 | 5.05, s | 131.0, CH |
| 20 | - | 134.3, qC |
| 21 | 2.45, br ddd (9.6, 7.4, 3.1) | 33.7, CH |
| 22α | 2.30, dd (13.9, 7.4) | 29.9, $CH_2$ |
| 22β | 1.85, m | - |
| 23 | - | 86.5, qC |
| 24 | - | 204.9, qC |
| 25 | 1.65, s | 16.8, $CH_3$ |
| 26 | 0.83, d (6.6) | 23.3, $CH_3$ |
| 27 | 1.05, d (6.6) | 19.8, $CH_3$ |
| 28 | 0.86, d (7.2) | 21.3, $CH_3$ |
| 29 | 1.27, s | 24.4, $CH_3$ |
| 30 | 1.72, s | 22.2, $CH_3$ |
| 31α | 1.98, ddd (13.2, 9.6, 4.8) | 33.6, $CH_2$ |
| 31β | 1.75, ddd (13.2, 10.5, 3.1) | - |
| 32 | 3.87, d (10.2, 4.8) | 73.3, CH |
| 33 | - | 82.5, qC |
| 34 | - | 212.8, qC |
| 35 | 2.21, s | 24.9, $CH_3$ |
| 36 | 1.21, s | 22.0, $CH_3$ |
| 1' | 4.41, d (6.0) | 103.6, CH |
| 2’ | 3.45, m | 74.6, CH |
| 3' | 3.45, m | 89.5, CH |
| 4' | 3.09, m | 74.9, CH |
| 5' | 3.27, m | 72.2, CH |
| 6’ | 1.24, d (6.6) | 18.2, $CH_3$ |
| 1" | 4.62, d (7.9) | 105.3, CH |
| 2” | 3.5, t (8.4) | 75.3, CH |
| 3” | 3.78, t (9.6) | 74.7, CH |
| 4” | 4.93, t (9.6) | 77.4, CH |
| 5” | 3.82, dd (9.6, 6.0) | 70.9, CH |
| 6” | 1.33, d (6.0) | 17.9, $CH_3$ |
| 7" | - | 168.0, qC |
| 8" | - | 122.6, qC |
| 9" | - | 155.6, qC |
| 11” | 7.35, d (8.4) | 132.6, CH |
| 10” | 6.85, d (8.4) | 116.2, CH |
| 12" | - | 125.7, qC |
| 13" | - | 135.7, qC |
| 14” | 2.41, s | 18.0, $CH_3$ |
| OH | 4.10 | - |
| OH | 3.92 | - |
| OH | 3.65 | - |

**Table S4. Cation and pH dependence of phocoenamicin MIC.** No significant changes above or below a two-fold dilution were observed.

| | **Phocoenamicin MIC ($\mu$M)** | **Vancomycin MIC ($\mu$M)** | **Daptomycin Mic ($\mu$M)** |
|---|---|---|---|
| **+0 mM Ca** | 3.5 | - | 11 |
| **+0.5 mM Ca** | 4.2 | - | 0.5 |
| **+1.25 mM Ca** | 4.2 | - | 0.1 |
| **pH 7.0** | 1.3 | 1.3 | - |
| **pH 6.0** | 0.63 | 0.78 | - |
| **pH 5.0** | 0.53 | 1.1 | - |

**Supplementary References**

(1) Tamura, K., Tamura, K., Nei, M., and Nei, M. (1993) Estimation of the number of nucleotide substitutions in the control region of mitochondrial DNA in humans and chimpanzees. *Mol. Biol. Evol. 10*, 512–526.
(2) Felsenstein, J. (1985) Confidence limits on phylogenies: an approach using the bootstrap. *Evolution 39*, 783–791.
(3) Tittensor, D. P., Mora, C., Jetz, W., Lotze, H. K., Ricard, D., Berghe, E. V., and Worm, B. (2016) Global patterns and predictors of marine biodiversity across taxa. *Nature 466*, 1098–1101.
(4) Tamura, K., Peterson, D., Peterson, N., Stecher, G., Nei, M., and Kumar, S. (2011) MEGA5: Molecular Evolutionary Genetics Analysis Using Maximum Likelihood, Evolutionary Distance, and Maximum Parsimony Methods. *Mol. Biol. Evol. 28*, 2731–2739.
(5) Ursell, T., Lee, T. K., Shiomi, D., Shi, H., Tropini, C., Monds, R. D., Colavin, A., Billings, G., Bhaya-Grossman, I., Broxton, M., Huang, B. E., Niki, H., and Huang, K. C. (2017) Rapid, precise quantification of bacterial cellular dimensions across a genomic-scale knockout library. *BMC Biol. 15*, DOI 10.1186–s12915–017–0348–8.